NAVAL POSTGRADUATE SCHOOL

Monterey, California

THESIS

DOPPLER SHIFT AND SPREAD STUDY FOR IONOSPHERICALLY PROPAGATED SIGNALS

by

Nickolaos Malachias

June, 1994

Thesis Advisor: Richard W. Adler

Approved for public release; distribution is unlimited

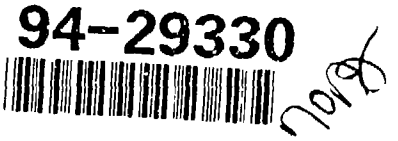

REPORT DOCUMENTATION PAGE

Form Approved
OMB No. 0704-0188

1. AGENCY USE ONLY (Leave Blank)	2. REPORT DATE	3. REPORT TYPE
	June, 1994	Master's Thesis

4. TITLE AND SUBTITLE
DOPPLER SHIFT AND SPREAD STUDY FOR IONOSPHERICALLY PROPAGATED SIGNALS

5. FUNDING NUMBERS

6. AUTHOR(S)
Malachias, Nickolaos

7. PERFORMING ORGANIZATION NAMES(S) AND ADDRESS(ES)
Naval Postgraduate School
Monterey, CA 93943-5000

8. PERFORMING ORGANIZATION

9. SPONSORING/MONITORING AGENCY NAME(S) AND ADDRESS(ES)

10. SPONSORING/MONITORING AGENCY REPORT NUMBER

11. SUPPLEMENTARY NOTES
The views expressed in this thesis are those of the author and do not reflect the official policy or position of the Department of Defense or the U.S. Government.

12a. DISTRIBUTION/AVAILABILITY STATEMENT
Approved for public release; distribution is unlimited

12b. DISTRIBUTION CODE

13. ABSTRACT (Maximum 200 words)

Modern, High Frequency (HF) communication techniques, such as spread spectrum and frequency hopping, require precise signal frequency information. The predominant HF propagation path is via the ionosphere, which often produces Doppler frequency shift and spread. This study examined the frequency spectra of selected HF signals traversing short and long mid-latitude paths and one high-latitude auroral zone path. Signal amplitude and Doppler shifts and spreads observed show diurnal, carrier frequency and ionospheric path dependencies. Higher frequency signals experienced more Doppler shift, especially during the daytime. Spectrum spreading was more pronounced at night and was affected by multiple reflections, the auroral oval and field-aligned ionization. Additional signal observations are needed to cover seasonal variations, disturbed ionospheric conditions and solar cycle variations. The impact of Doppler shift and spread on wide-spectrum HF communications also needs to be examined.

14. SUBJECT TERMS	16. PRICE CODE
Doppler Shift, Doppler Spread, HF Signals, LUF, MUF.	15. NUMBER OF PAGES 71

17. SECURITY CLASSIFICATION OF REPORT	18. SECURITY CLASSIFICATION OF THIS PAGE	19. SECURITY CLASSIFICATION OF ABSTRACT	20. LIMITATION OF ABSTRACT
Unclassified	Unclassified	Unclassified	UL

NSN 7540-01-280-5500 Standard Form 298 (Rev. 2-89)

Approved for public release; distribution is unlimited.

DOPPLER SHIFT AND SPREAD STUDY FOR IONOSPHERICALLY PROPAGATED SIGNALS

by

Nickolaos Malachias
LTJG, Helenic Navy
BS, Helenic Naval Academy, 1986

Submitted in partial fulfillment
of the requirements for the degree of

MASTER OF SCIENCE IN ELECTRICAL ENGINEERING

from the

NAVAL POSTGRADUATE SCHOOL
June, 1994

Author: _____
Nickolaos Malachias

Approved By: _____
Richard W. Adler, Thesis Advisor

_____
Wilbur R. Vincent, Second Reader

_____
Michael A. Morgan, Chairman
Department of Electrical and Computer Engineering

ABSTRACT

Modern, High Frequency (HF) communication techniques, such as spread spectrum and frequency hopping, require precise signal frequency information. The predominant HF propagation path is via the ionosphere, which often produces Doppler frequency shift and spread. This study examined the frequency spectra of selected HF signals traversing short and long mid-latitude paths and one high-latitude auroral zone path. Signal amplitude and Doppler shifts and spreads observed show diurnal, carrier frequency and ionospheric path dependencies. Higher frequency signals experienced more Doppler shift, especially during the daytime. Spectrum spreading was more pronounced at night and was affected by multiple reflections, the auroral oval and field-aligned ionization. Additional signal observations are needed to cover seasonal variations, disturbed ionospheric conditions and solar cycle variations. The impact of Doppler shift and spread on wide-spectrum HF communications also needs to be examined.

TABLE OF CONTENTS

I. INTRODUCTION

Modern communication techniques, such as spread spectrum and frequency hopping, require precise knowledge of the frequency spectrum of the signals. Ionospherically propagated High Frequency (HF) signals generally experience a Doppler frequency shift and spread which degrades the effectiveness of systems that require precise signal frequency information. The main factor which causes Doppler shift is the vertical motion of the ionospheric layers due to the change in electron density. Also, if anomalies occur during the reflection of the wave from the ionospheric layers, the signals suffer from frequency spread. In order to study Doppler shift and spread, frequency measurements were taken at the Naval Postgraduate School, Monterey, CA during the period 05 April 1994-10 May 1994. The transmitting stations and frequencies monitored were :

- WWV, Ft. Collins, CO (5 MHz, 10 MHz, and 15 MHz)
- BBC Relay Station, New Brunswick, Canada (6,175 kHz)
- BBC Relay, Ascension Island, South Atlantic Ocean (15,260 kHz)
- Naval Station NAF, Cape Wales, AK (16,804 kHz)

After that, received data was tabulated and plotted for each particular frequency, showing amplitude, Doppler shift and spread variations. An attempt was then made to explain the data variations from ionospheric theory, considering factors such as

frequency, and the date of observation (which identifies the ionospheric condition). Charts showing the auroral oval for the measurement dates along with the signal path were also employed (see Appendix). The auroral oval determines areas where significant signal disturbances are expected due to corresponding ionospheric anomalies. Auroral oval charts were obtained using the ADVANCED PROPHET Program, version 4.3.

Data for this effort was obtained with standard laboratory instruments and equipment. Specialized receiving and data-processing were not used. This rather simplistic approach for Doppler shift and spread measurements was possible because of recent advances in digital instrumentation and stable synthesized receivers.

II. THEORETICAL BACKGROUND

A. THE IONOSPHERE

The ionosphere is the area of the atmosphere which extends from about 50 km out to several earth radii (the mean radius of earth is about 6371 km). In terms of effects on radio wave propagation, it is effective only out to about 500 km.

The ionosphere is divided into three regions (layers), which are the D, E and F-layers. During the day, the F-layer splits into the F_1 and F_2, with the F_2 being the higher and denser of the two, as seen in Figure 1.

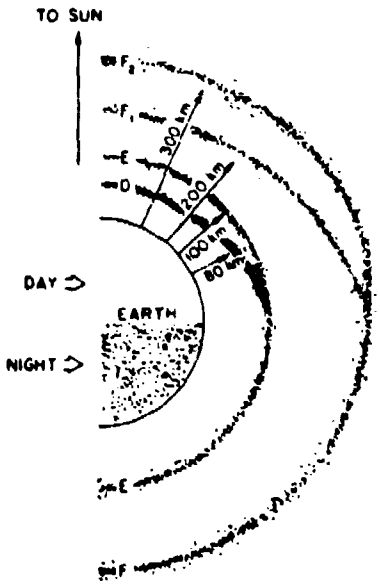

Figure 1. Ionospheric Regions (Ref. 1).

Typical density versus altitude values are in Figure 2. From these two figures, the height of peak density, h_m, for daytime can be seen to be approximately 100 km for the E-layer, while the peaks of F_1 and F_2 are 200 km and 300 km respectively The E and F-layers are reflective layers, whereas the D-layer is absorptive and attenuates signals passing through it.

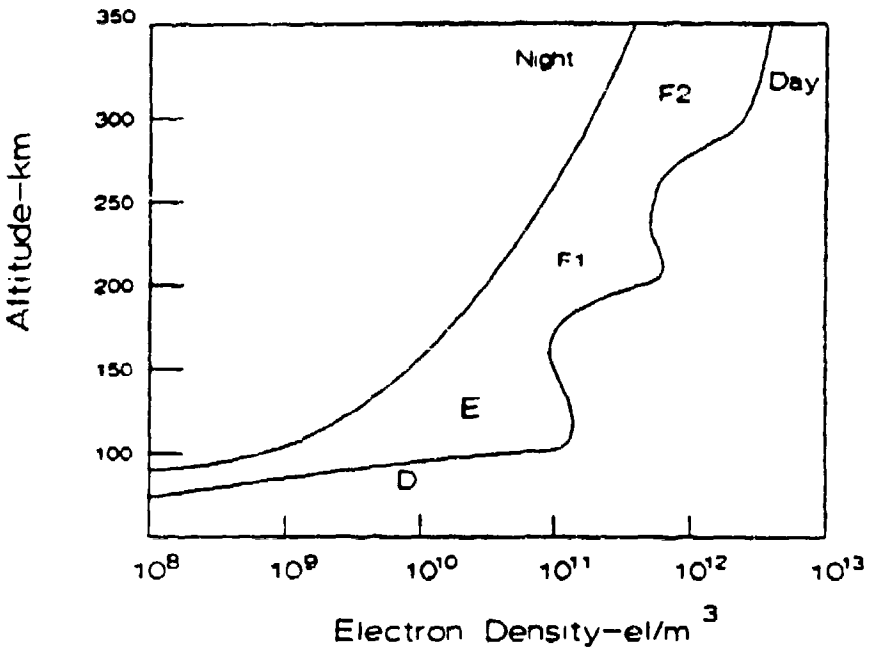

Figure 2. Typical Electron Distribution in the Ionosphere (Ref. 2).

If a plane wave is vertically incident on the ionosphere from below, it will interact with the ionized layers and will be reflected from a level at which the refractive index n= 0. In general it is:

$$n = [1 - (f_p/f)^2]^{1/2}, \quad (1)$$

where f_p is the plasma (resonance) frequency and f is the radiowave frequency.

The plasma frequency is defined for any point in the ionospheric plasma and is proportional to the square root of the electron density,

$$f_p = 9N_e^{1/2}, \quad (2)$$

where f_p is in Hz and N_e is in electrons/m^3. For a typical E-layer electron density of 10^{11}, $f_p = 2.85$ MHz.

From Equation 1, the reflection of the plane wave occurs at the point where the radio frequency matches the local plasma frequency. If the layer has a defined peak in electron concentration N_{max}, then the corresponding plasma frequency profile will also have a maximum. The maximum plasma frequency in the layer (having a distinct peak) is called the critical or penetration frequency f_c (or f_0).

1. D-Layer

The ionization of the D-layer is controlled by solar radiation. It builds up rapidly at sunrise, reaches a maximum near noon, quickly diminishes at sunset, and finally disappears completely at night. It extends from about 50 km to 90 km, but blends in with the E-layer at the upper end, with no discrete boundary between them. Because of its low electron density, the D-layer absorbs HF radio waves. Typical values of midday ionospheric absorption can be seen in Figure 3.

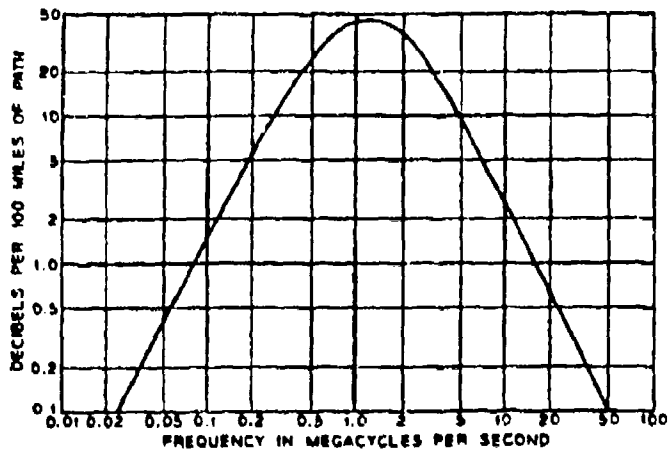

Figure 3. Typical Values of Midday Ionospheric Absorption (Ref. 3).

From plasma theory, a propagating wave loses energy during plasma interaction. This occurs in the D-layer, where the probability of collisions increases with decreasing frequency. This frequency dependence leads to the concept of a "lowest usable frequency" or LUF. For a given transmitter power and antenna gain, the lowest frequency which can be received with usable signal strength is defined as the LUF and will be dependent upon the D-layer characteristics.

2. E-layer

The E-layer extends from the top of the D-layer to the bottom of the F-layer or from approximately 90 - 130 km and peaks sharply at about 100 km. Like the D-layer, the E-layer is greatly influenced by solar radiation. It is the most predictable of the ionospheric layers.

Each layer has its own critical frequency. To describe solar control over layer formation, the solar zenith angle χ will be defined. This is the angle between the local normal and the sun's position, shown in Figure 4.

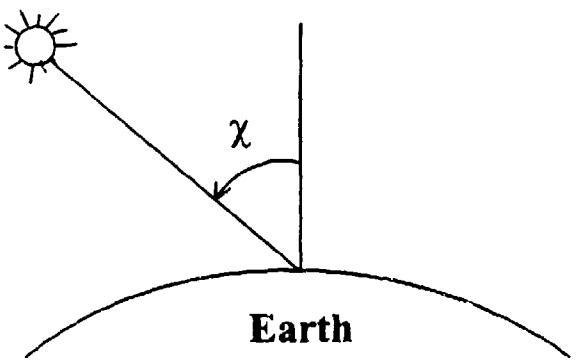

Figure 4. Solar Zenith Angle.

From the solar zenith angle an approximation for the E-layer critical frequency, f_0E, is

$$f_0E\ (MHz) = 0.9[(180 + 1.44R)\cos\chi]^{1/4}, \qquad (3)$$

where R is the Wolf of Zurich sunspot number.[1] This equation is very accurate during the daylight portion of the day. During the night the E-layer does not disappear completely but f_0E reaches a minimum of about 0.25 MHz at sunspot minimum and 0.5 MHz at sunspot maximum. Typical daily noon values of f_0E are in the range of 3-4 MHz. The

[1] An index of solar activity, the Wolf of Zurich sunspot number is defined as follows: R=K(10q+S); q is the number of sunspot groups; S is the number of individual sunspots, and K is a correction factor which depends on the particular observatory.

maximum frequency that would be reflected from a plasma in terms of the critical frequency and the incident angle, ϕ, of the wave is

$$f_{max} = f_c \sec\phi. \tag{4}$$

This is accurate for a flat earth but requires a minor modification for a curved earth and curved ionosphere. The modification is a correction factor, k, which varies from 1.0 to 1.2 for most cases and is a function of the reflection height and the distance. A factor of 1.1 can be assumed for most cases. Equation (4) then becomes

$$f_{max} = k f_c \sec\phi = 1.1 f_c \sec\phi. \tag{5}$$

For ionospheric propagation, this f_{max} or maximum frequency takes on a special name which is the "maximum usable frequency" or MUF. Because of the curvature of the earth and the ionosphere, at the lowest launch angle of 0° elevation angle, ϕ will be approximately 74°. The maximum MUF will then be

$$\text{MUF(max)} = k f_c \sec 74^\circ = 3.6 f_c. \tag{6}$$

If the noon f_0E is 4 MHz, the highest frequency reflected from the E-layer or MUF (E) would be approximately 14 MHz.

3. F-Layer

The highest, thickest, and densest layer is the F-layer. Due to its higher density, its critical frequency is higher than that of the E-layer. It extends upwards from the E-layer at about 130 km. During the daytime, the F-layer normally splits into the F_1 and the F_2. The F_1 is lower and less dense than the F_2, and like the D and E-layers, is controlled by solar activity and is only apparent during the daytime. It spans from the

E-layer to the F_2 layer with a peak normally around 200 km. Although not as predictable as the E-layer, its critical frequency is approximately

$$f_0F_1(\text{MHz}) = (4.3 + 0.1R)\cos^{0.2}\chi. \quad (7)$$

The most important layer for HF communications is the F_2. Its daytime peak height of about of about 300 km permits longer transmission distances. Unfortunately, it is the least predictable. Published maps, or huge data bases, which are both derived from historical data, are normally used to predict the f_0F_2. The F_2 does not follow direct solar control as closely as the other layers. It does not disappear at night but does decrease in density.

B. DOPPLER THEORY

1. Doppler Fundamentals

The Doppler effect, first noted with sound waves, is the difference between the transmitted frequency and the received frequency, caused by relative motion between the transmitter and receiver. Assume a sinusoidal signal, S(t), of constant amplitude and frequency, transmitted from a stationary source and received T seconds later. The received signal is

$$S(t-T) = A\cos[2\pi f(t-T)]. \quad (8)$$

If the delay varies as a function of time,

$$T = g(t). \quad (9)$$

and thus

$$S(t-T) = A\cos\{2\pi f[t-g(t)]\}. \quad (10)$$

In the case of an approaching sound source, the delay is a function of the distance, d, and the velocity of the signal in the transmission medium, V_p. In this case, V_p is the speed of sound. The delay, g(t), is therefore

$$g(t) = d/V_p = d(t)/V_p, \quad (11)$$

since the distance varies with time. The distance varies as a function of the speed V_s, and is therefore

$$d(t) = -V_s t. \quad (12)$$

Finally,

$$S(t-T) = A\cos\{2\pi f[t-g(t)]\} = A\cos[2\pi ft(1+V_s/V_p)]. \quad (13)$$

The change in frequency, or Doppler shift is

$$f_D = f(1 + V_s/V_p) - f = f(V_s/V_p). \quad (14)$$

This Doppler equation applies to electromagnetic waves as well as sound waves. V_p becomes the speed of light, C, and f usually is the radiowave frequency.

2. Ionospheric Doppler

If the ionospheric layer moves in the vertical direction with velocity V_s as shown in Figure 5, then equation (14) becomes

$$f_D = f(V_s/V_p)\cos\phi \quad (15)$$

where V_p is the speed of light and ϕ is the angle between the receiver line-of-sight to the reflection point and the line normal to that point.

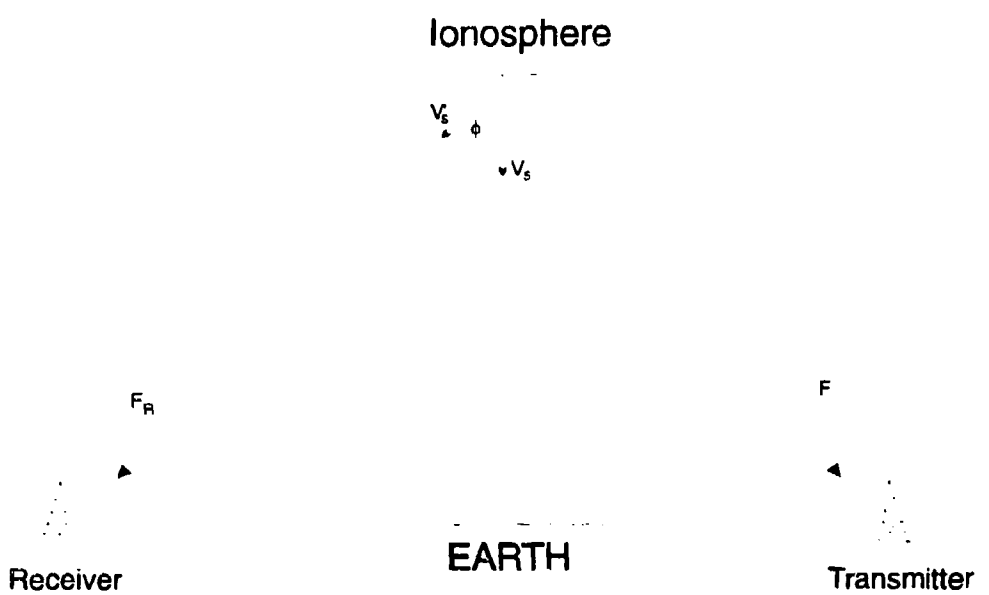

Figure 5. Vertical Ionospheric Movement.

Movement in the horizontal direction sets up a horizontal electron density distribution. Horizontal distributions are called "tilts", and the major consequence of those is to cause "non-great circle" propagation.

If the layer descends, as shown in Figure 6, the virtual height descends a proportional amount and the group path, P, from transmitter to receiver becomes shorter. The Doppler shift is thus proportional to the path length change.

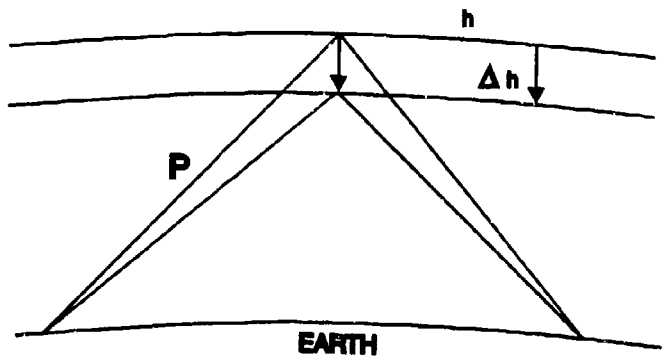

Figure 6. Virtual Height Changes with Descending Layer.

Analogous to this situation, is when the electron density beneath the layer increases, lowering the reflection height, with a similar decrease in the group path. With respect to the propagating wave, the two actions are indistinguishable, and a Doppler shift likewise occurs for a change in electron density of the layer.

III. EXPERIMENTAL PROCEDURE

A. GENERAL SETUP

In order to observe the Doppler shift and spread of various HF ionospherically propagated signals, measurements were taken from 4/5/94 to 5/10/94 either at room 216 of Spanagel Hall or at Building 218 (Beach site) of NPS. In both cases, the experimental set up of Figure 7 included a dipole or a long-wire antenna, the ICOM IR-9000 Receiver, and the HP 3561A spectrum analyzer.

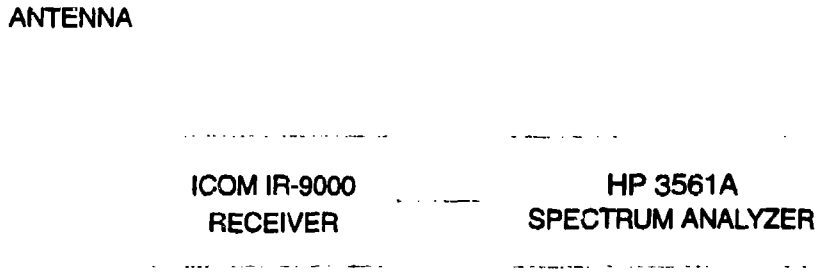

Figure 7. Experimental Set-up.

The HP 3561A is a single-channel, Fast-Fourier Transform (FFT) signal analyzer covering 0 to 100 kHz. In order to observe the carrier frequency of a received signal, the beat frequency oscillator (BFO) of the receiver was tuned 1-kHz below the actual carrier

frequency. This translates the carrier frequency downward into a 1-5 Hz audio tone. The precise frequency of the audio tone was then measured by the HP 356A Analyzer.

B. STATION LIST

The stations monitored for frequency spectrum measurements were WWV-CO, BBC-Relay Canada, BBC Relay-Ascension Island, and Cape Wales Naval Station-AK. The characteristics of the above stations are shown in Table I. Figure 8 also shows the location of these stations on a great circle map centered on Monterey.

TABLE I. CHARACTERISTICS OF THE TRANSMITTING STATIONS

STATION	LOCATION	FREQUENCY	POWER	TYPE OF ANTENNA
WWV	Ft. Collins, CO, USA	5 MHz 10 MHz 15 MHz	10 kW	Center Fed Half Wavelength Vertical
BBC Relay	Sackville, Canada South Atlantic Ocean Ascension Isl.	6175 kHz 15260 kHz	250 kW 250 kW	Curtain Antenna
Cape Wales Naval Station (NAF)	Cape Wales, AK	16,804 kHz	100 W	Dipole Antenna

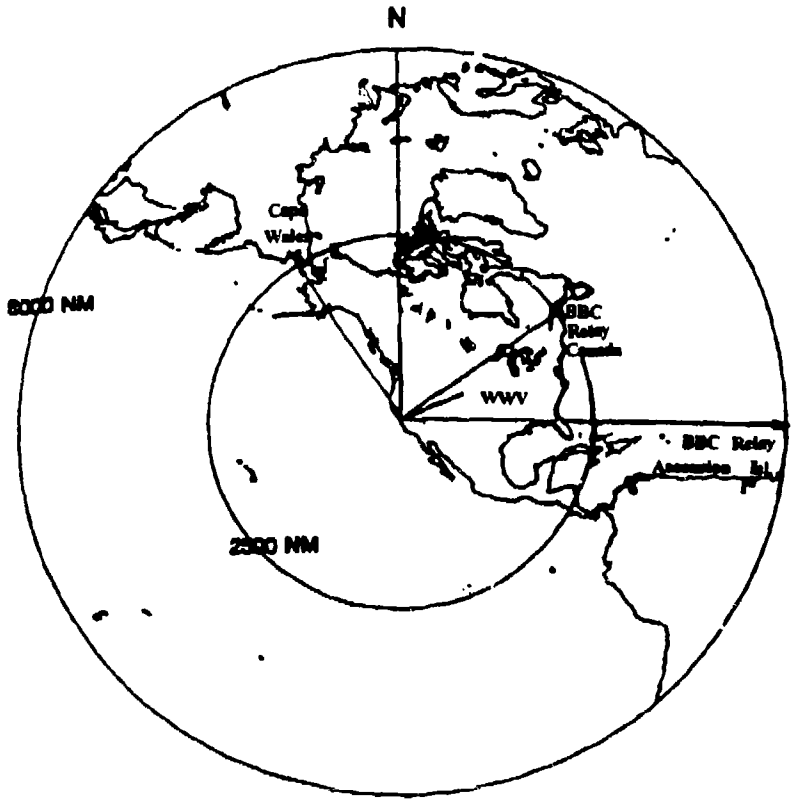

Figure 8. Location of the Transmitting Stations.

IV. EXPERIMENTAL RESULTS

A. 14,999 kHz WWV OBSERVATIONS

A set of typical frequency spectrum observations from WWV at 14,999 kHz, shown in the following figures, show amplitude, shift, and spread of the signal. Frequency shift from left to right is termed a "positive" shift, while movement from right to left is "negative." For the signal spread, a 6 dB bandwidth was observed and called the "6 dB spread." Figure 9 covers the period from 0631 to 1257 hours on 5/1/94. A second spectral component appears slightly higher in the frequency than the primary component. This component is from a second path using a different reflection point than the primary component. There is also a significant shift of this component from left to right as the day progresses. This is due to the downward movement of the ionospheric region, caused by an increase in the electron density. At 0748 and 1257 hours, more than one spike appears. This is because, in some cases, the wave is split into multiple paths while reflecting off ionospheric layers. Figure 10 shows the signal strength typically peaking around noon, while the frequency shift is still in progress. At 1219 hours, two spectral components again appear.

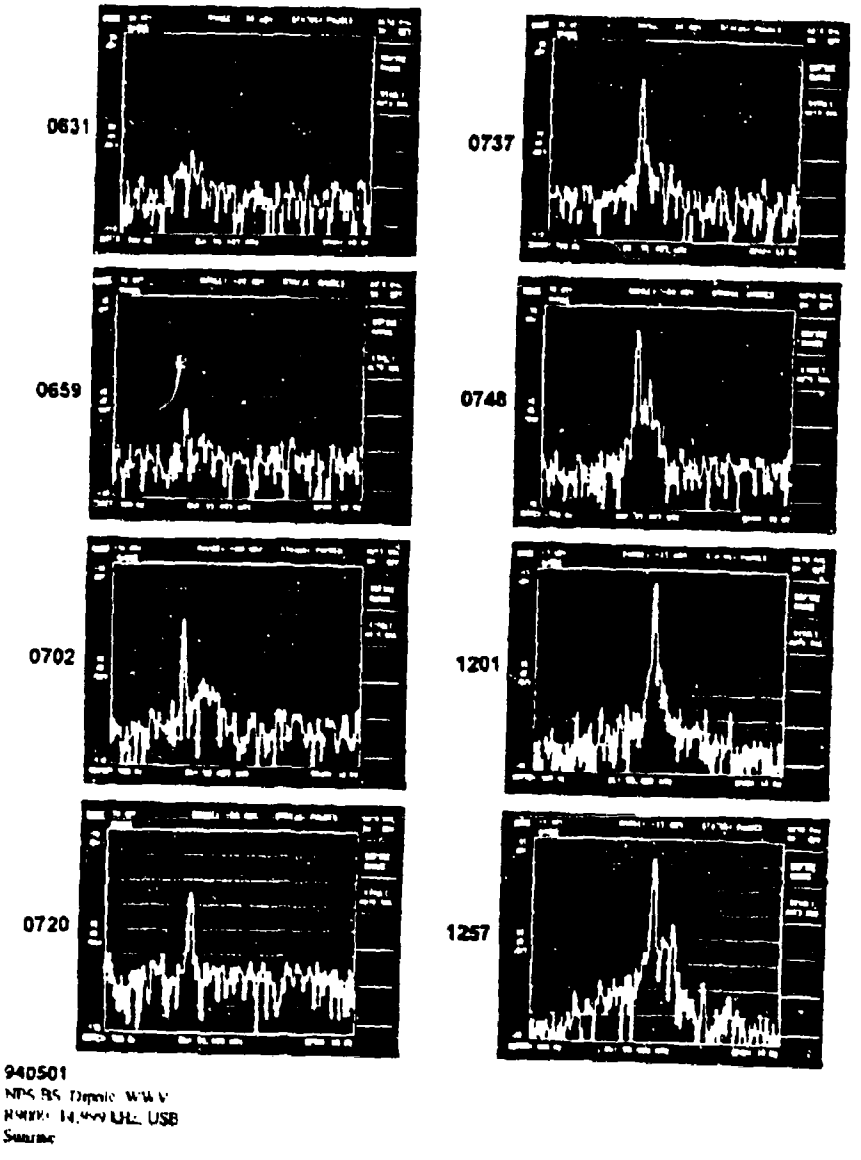

Figure 9. WWV Observations at 14,999 kHz on 1 May 1994.

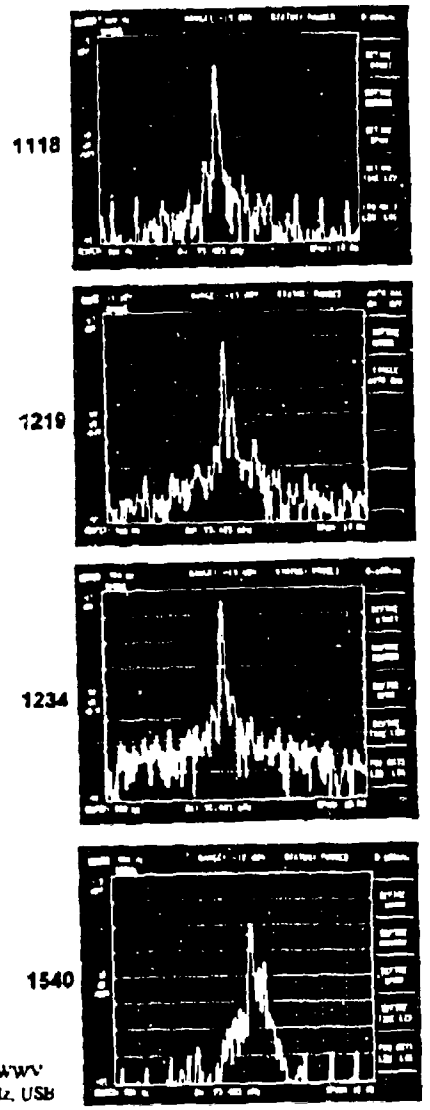

Figure 10. WWV Observations at 14,999 kHz on 4 May 1994.

From 1207 to 1649 on 4/28 the signal amplitude experiences an attenuation of approximately 20 dB as is shown at Figure 11. The total frequency shift is about 1.5 Hz; at 1649 hours, a 6 dB spread of about 2.0 Hz occurs.

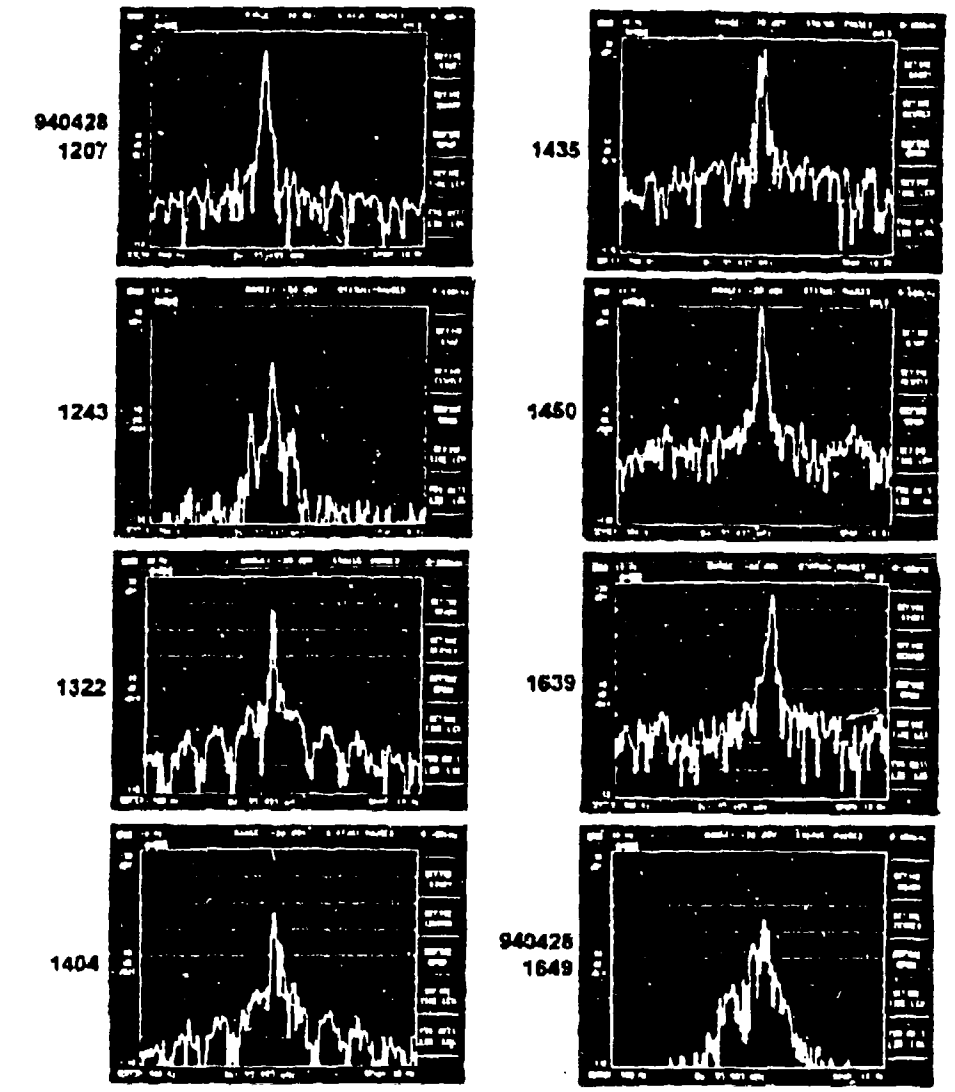

Figure 11. WWV Observations at 14,999 kHz on 28 April 1994.

As is shown in Figure 12, from 1721 hours on 4/28 to 0249 hours on 4/29 the signal amplitude decreases by 14 dB, starting at a value of about -56 dBV at 1721 hours. At 1929 hours, the signal reaches a peak value of -17 dBV. At 2005 hours, two additional spectrum components appear to the right of the carrier. As time progresses, the signal becomes weaker, while the total frequency shift is negligible. The maximum value of 6 dB spread is about 3.3 Hz, at 1956 hours, while the minimum value is about 1.0 Hz, at 1929 hours.

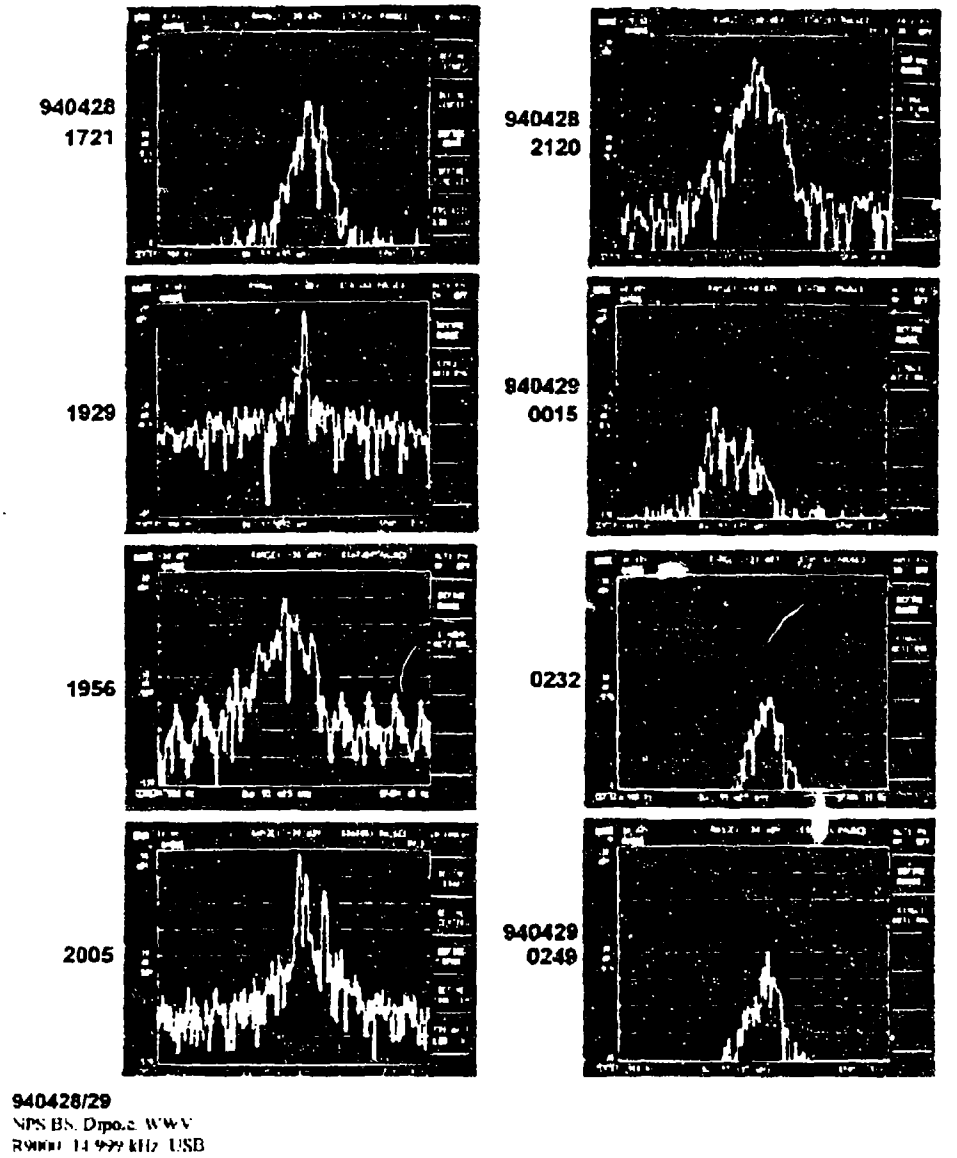

Figure 12. WWV Observations at 14,999 kHz on 28-29 April 1994.

Figure 13 shows the signal data for the period between 0323 and 0652 hours on 4/29. Through the period, the signal amplitude increases by about 8 dB, while the

maximum value is -62 dBV at 0525 hours. The maximum 6 dB spread was obtained at 0623 hours, and was about 1.7 Hz. The minimum spread, obtained at 0434, was about 0.7 Hz. The total frequency shift observed was negative 4 Hz.

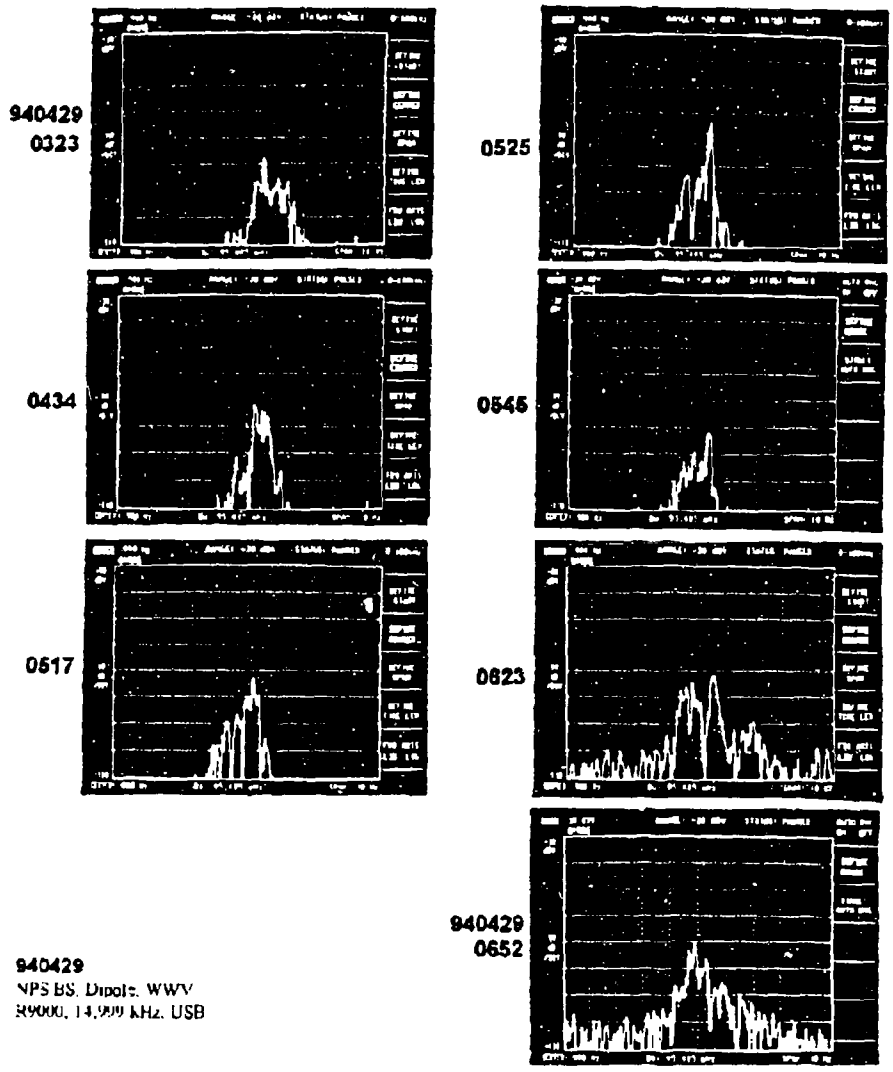

Figure 13. WWV Observations at 14,999 kHz on 29 April 1994.

Table II contains observed data for 4/28-29, while Figures 14, 15, and 16 show amplitude, Doppler shift, and spread variation versus time. The data demonstates that:

- The signal amplitude is high during the daytime, reaching values as high as -34 dBV around noon. At night, the signal is much weaker, reaching values as low as -80 dBV.
- The signal shifts significantly in the positive direction during the daytime, while at night the shift is less.
- The frequency spectrum is narrow during the day, spreading more in the evening. During the night, the spread does not change significantly, maintaining an average value of 1.5 Hz.

TABLE II. DATA RECEIVED FROM WWV (14.999 kHz) ON 28-29 APRIL 1994			
Time	Amplitude (dBV)	Doppler Shift (Hz)	6 dB Doppler Spread (Hz)
1207	-34	Reference	0.7
1243	-50	0.3	1.5
1322	-42	0.6	0.7
1404	-52	0.9	0.5
1435	-33	1.0	0.7
1450	-30	1.2	0.8
1639	-46	1.8	0.9
1649	-55	1.6	1.0
1721	-56	1.5	1.6
1929	-17	1.3	0.6
1956	-40	0.8	3.0
2005	-31	1.0	1.8
2120	-39	0.9	2.2
0015	-79	1.0	2.0
0223	-78	1.5	1.3
0249	-70	1.4	1.0
0323	-78	1.3	1.5
0434	-71	1.0	0.8
0517	-72	1.1	1.5
0525	-62	1.0	1.2
0545	-81	1.1	1.4
0623	-71	1.3	1.7
0652	-70	0.9	2.0

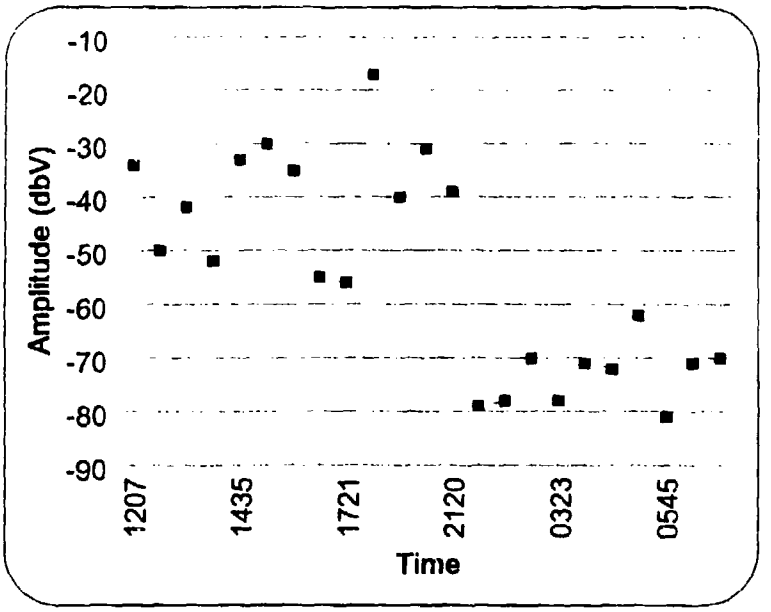

Figure 14. Amplitude vs Time Plot from WWV (14,999 kHz) on 28-29 April 1994.

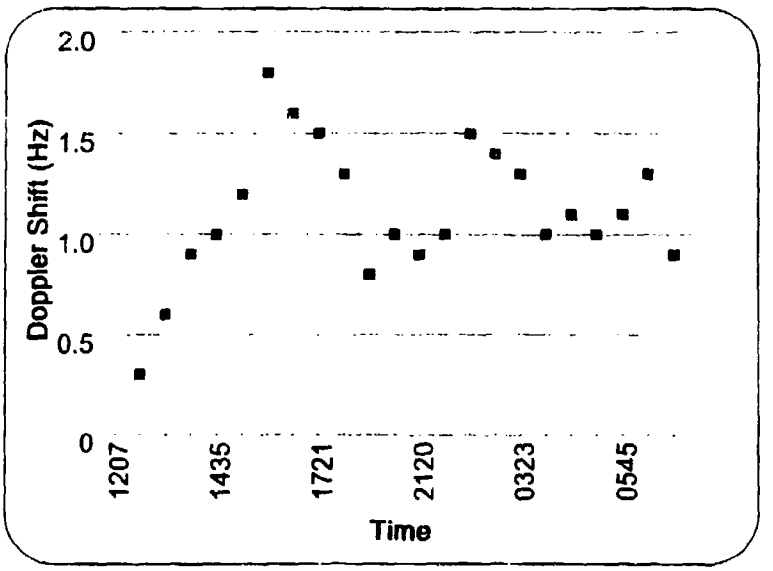

Figure 15. Doppler Shift vs Time Plot from WWV (14,999 kHz) on 28-29 April 1994.

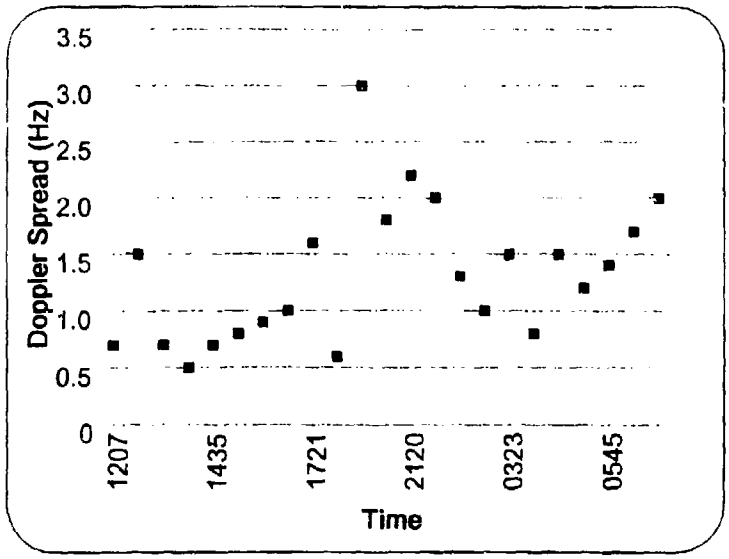

Figure 16. Doppler Spread vs Time Plot from WWV (14,999 kHz) on 28-29 April 1994.

B. 9,999 kHz WWV OBSERVATIONS

The next set of observations from WWV, CO was at 9,999 kHz. Figure 17 shows measurements made at about sunrise on 5/1. The figure shows a primary spectral component that grows as time progresses, similar to the observed behavior at 14,999 kHz. Over the period, the signal amplitude experiences an increase of about 16 dB while the total frequency shift is positive, with a value of about 0.8 Hz. Also, the average 6 dB spread is approximately 3.5 Hz.

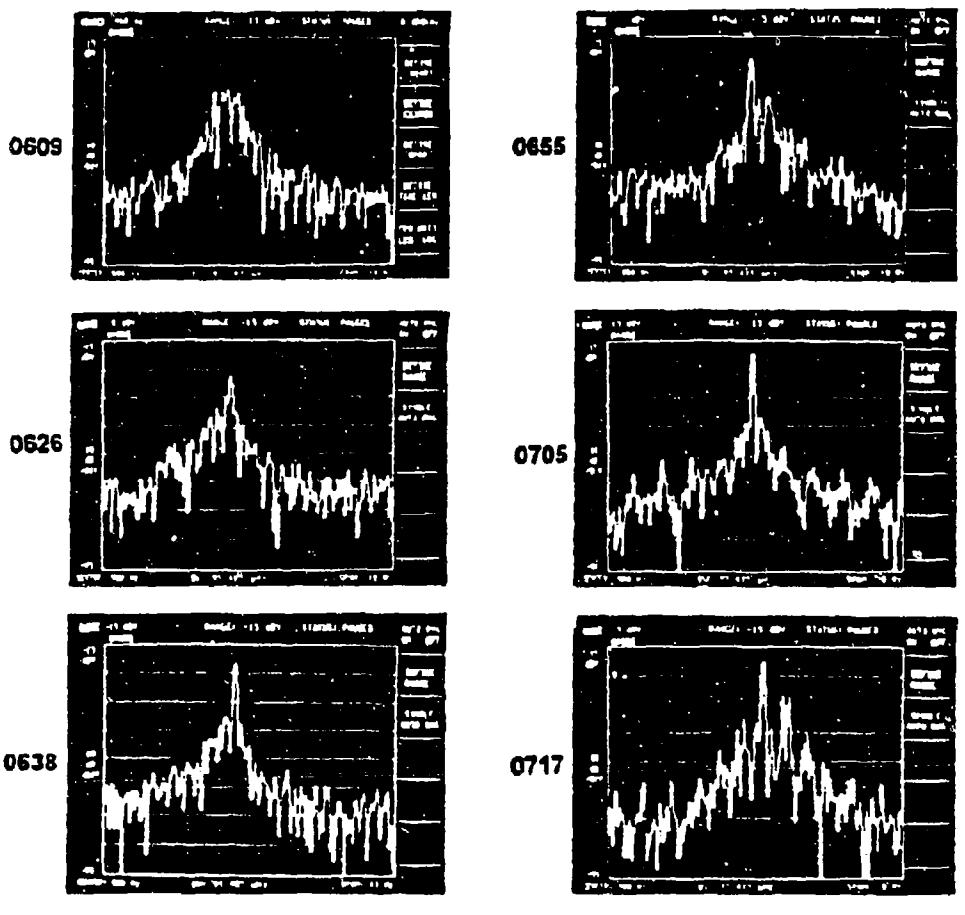

Figure 17. WWV Observations at 9,999 kHz on 1 May 1994.

Figure 18 shows the spectra obtained between 1119 and 1541 hours on 5/4. During the period, the signal amplitude does not show significant variation, reaching a high of

almost -15 dBV. The total frequency shift is about 0.6 Hz, while the maximum spread is 2.0 Hz, obtained at 1205 hours.

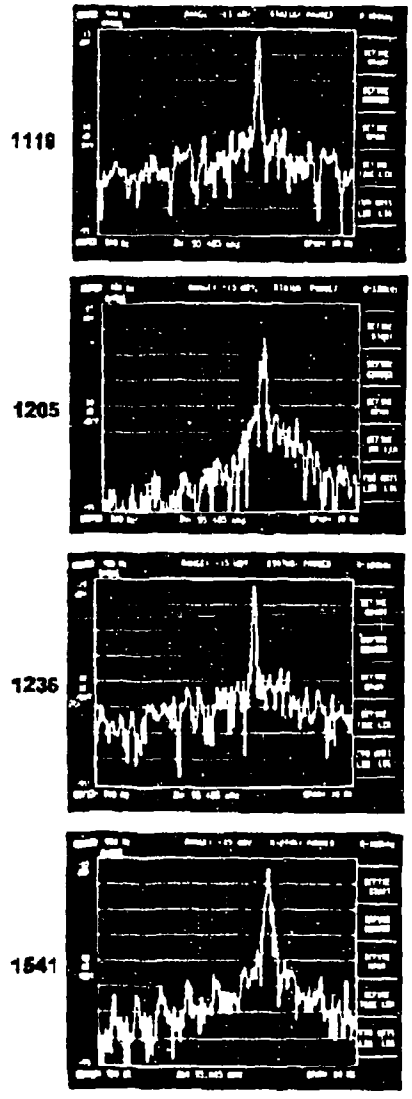

Figure 18. WWV Observations at 9.999 kHz on 4 May 1994.

The data obtained from 1216 to 1947 hours on 4/30, is presented in Figure 19. The signal amplitude is almost constant throughout the period, with an average value of about -19 dBV. The total frequency shift is 10 Hz. From 1533 to 1851 hours, additional spectral components appear around the carrier. The sources of these components is not known; however, they do not appear to be from ionospheric effects. The spread of the signal does not vary significantly and has an average value of 2.0 Hz.

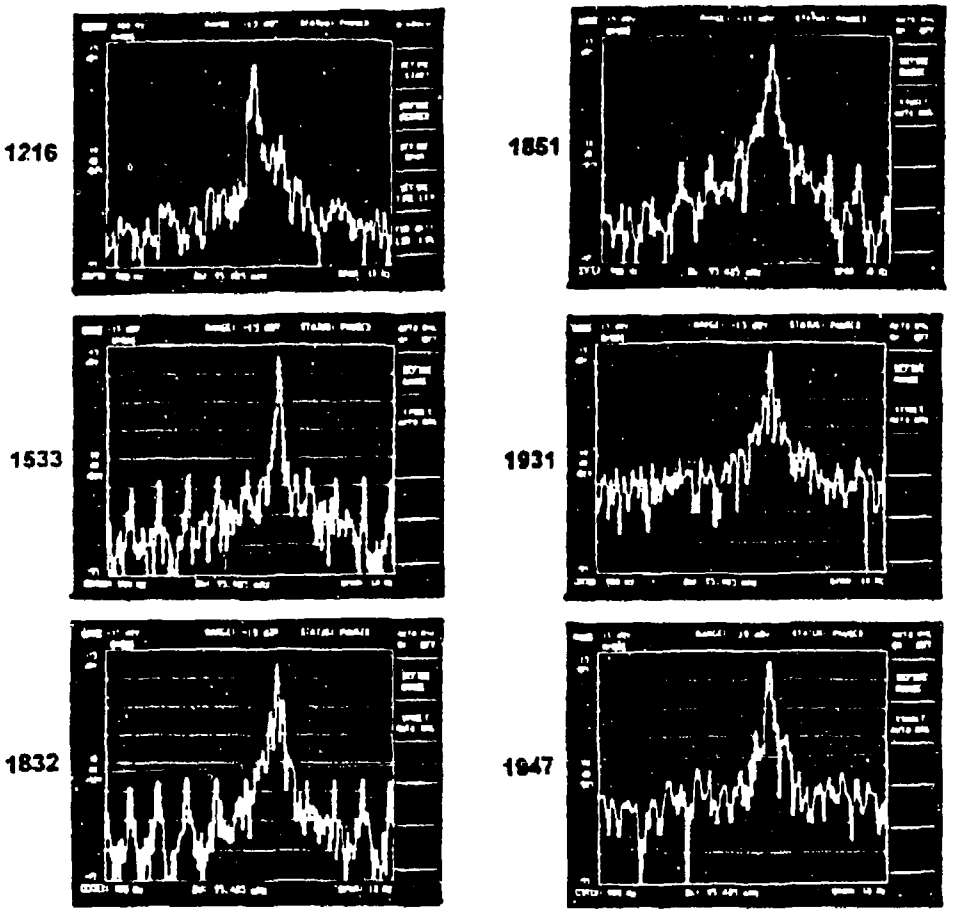

Figure 19. WWV Observations at 9,999 kHz on 30 April 1994.

Figure 20 shows the spectra obtained from 1209 to 1651 hours on 4/28. The signal amplitude varies slightly, with an average value of -40 dBV, while the total amount of the

frequency shift is positive 1.0 Hz. Additional spectral components also appear around the carrier for most of the period. The signal spread varies in range. from 0.7 to 2.0 Hz.

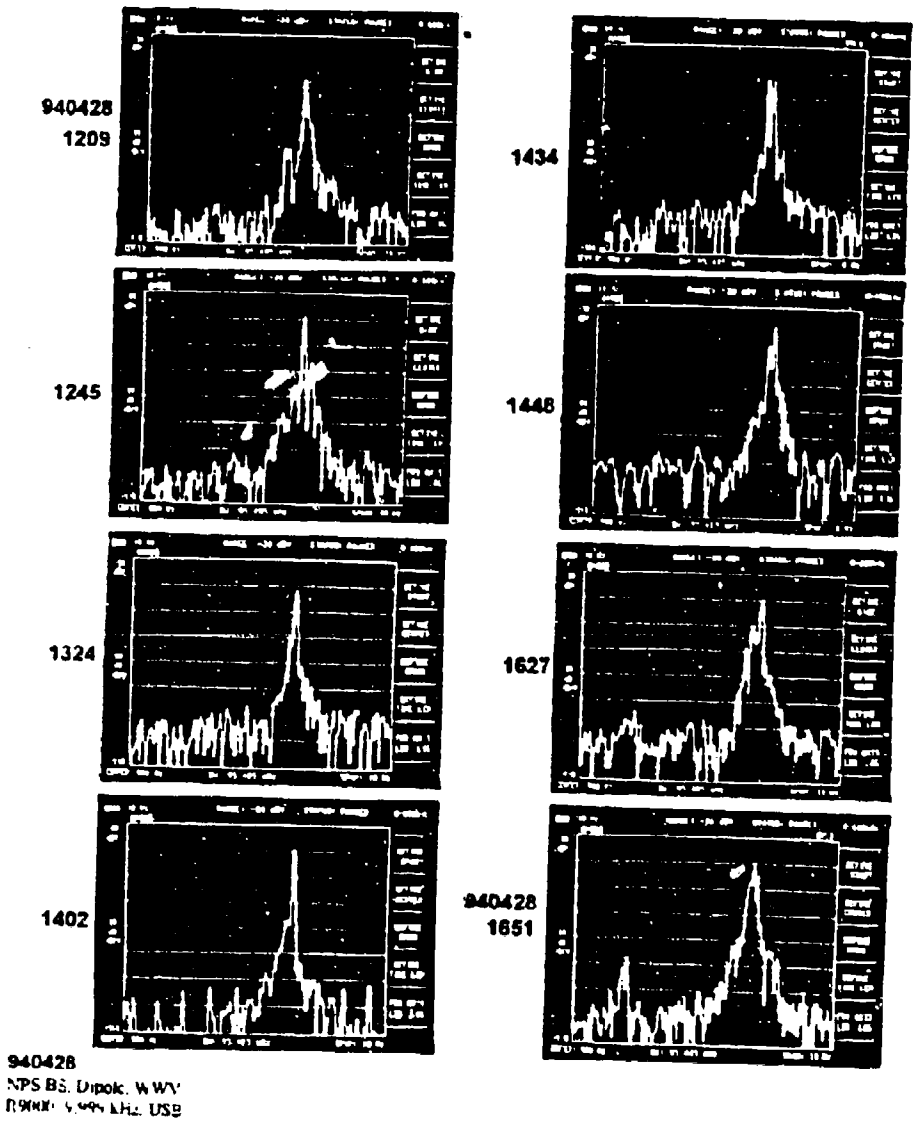

Figure 20. WWV Observations at 9,999 kHz on 28 April 1994.

Figure 21 illustrates the spectra for the period from 1715 hours on 4/28 to 0220 hours on 4/29. Over the period, the signal amplitude experiences a total attenuation of 20 dB. The total frequency shift is negative 0.5 Hz. The signal becomes more spread after midnight, with an average 6 dB value of 2.2 Hz.

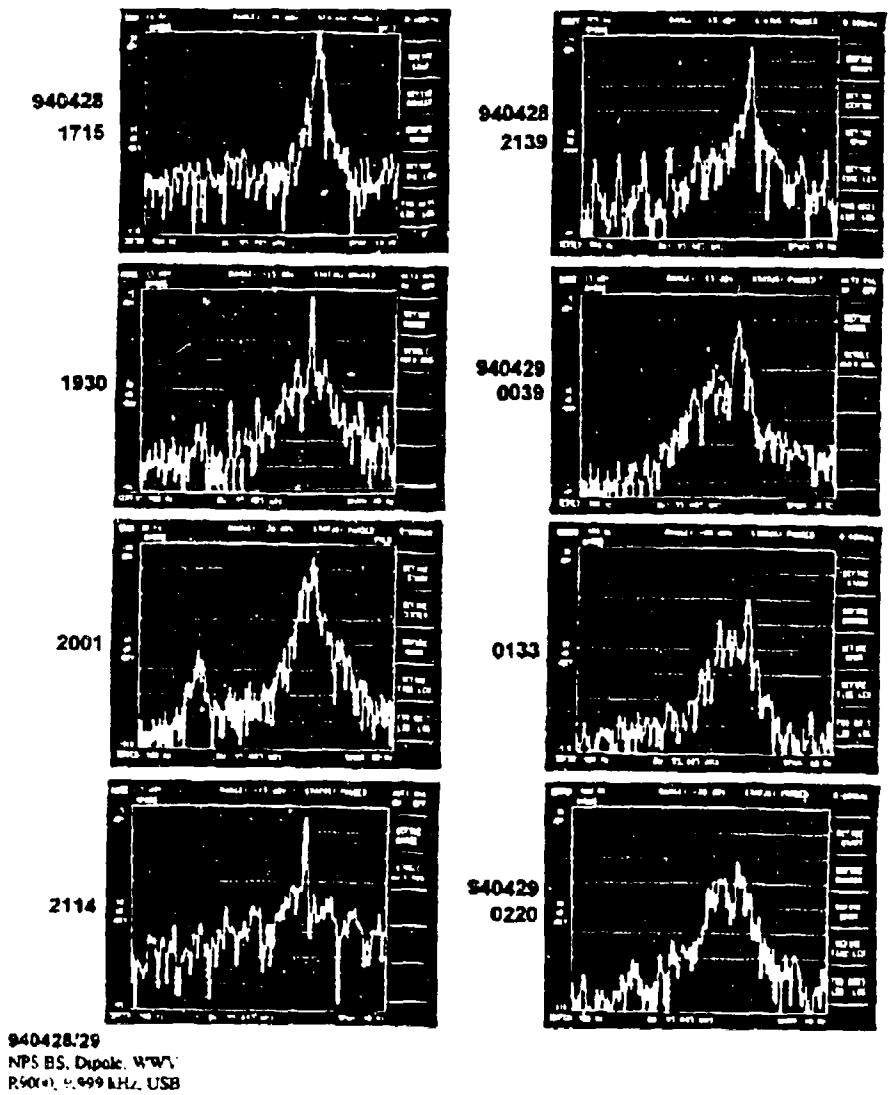

Figure 21. WWV Observations at 9,999 kHz on 28-29 April 1994.

In Figure 22 for 0245 to 0650 hours on 4/29, the signal amplitude increases about 30 dB, while the frequency shift is negative at about 0.7 Hz. The signal spread decreases as time progresses, starting at 4.0 Hz and ending at 1.2 Hz.

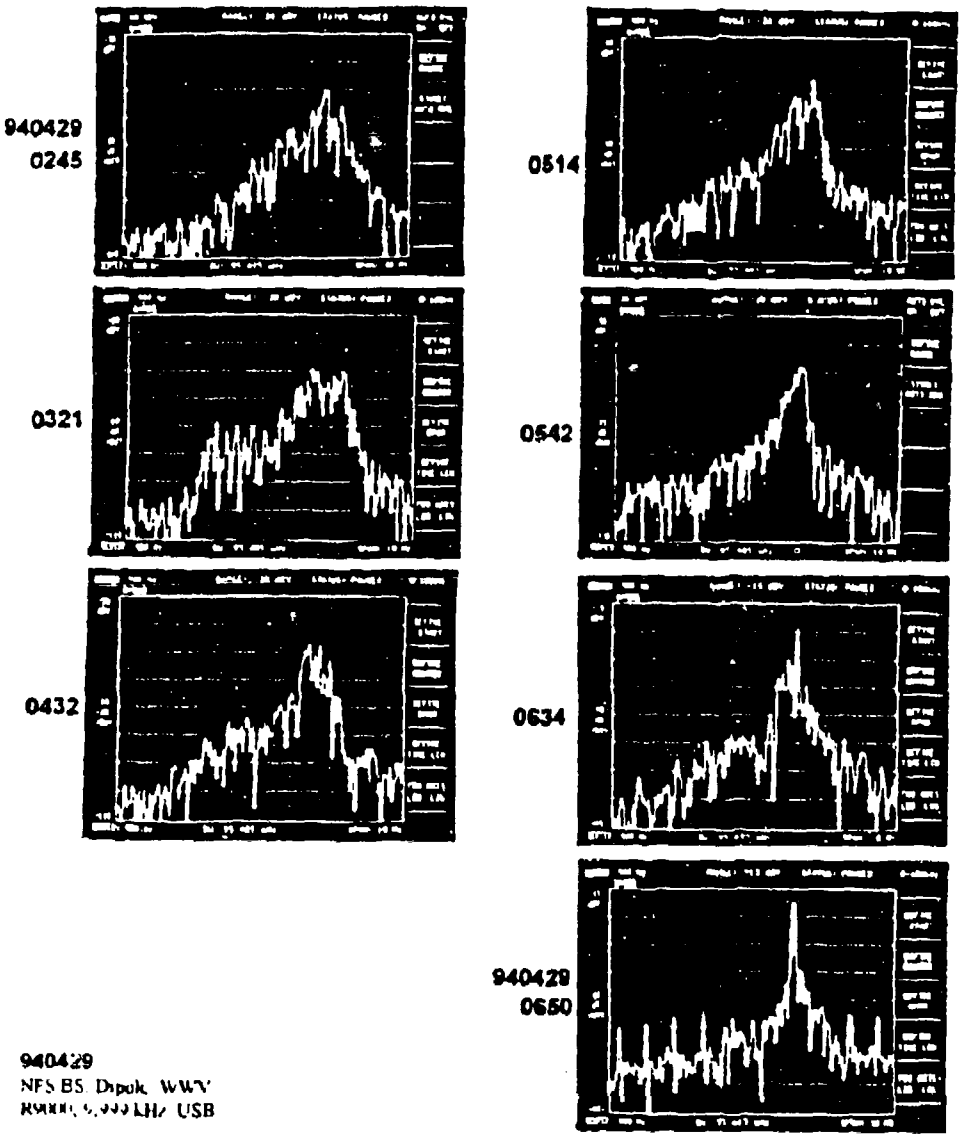

Figure 22. WWV Observations at 9,999 kHz on 29 April 1994.

Table III summarizes the measured data for 4/28-29. Figures 23, 24, and 25 show amplitude, shift, and spread variation versus time. In summary:

- The signal amplitude is -48 dBV around noon. At night, the signal is weaker, but levels are generally higher than those for 14,999 kHz.
- The signal frequency shifts in a positive direction during the daytime, while by late afternoon, it starts shifting in a negative direction, until the next sunrise.
- The signal spectrum is more spread during the nighttime, narrowing after sunrise.

TABLE III. DATA REC[illegible]VED FROM WWV (9,999 kHz) ON 28-29 APRIL 1994.			
Time	Amplitude (dBV)	Doppler Shift (Hz)	6 dB Doppler Spread (Hz)
1209	-48	Reference	1.0
1245	-39	0.1	1.1
1324	-41	0.2	0.7
1402	-40	0.4	0.6
1434	-42	0.4	1.0
1448	-38	0.8	1.1
1627	-40	0.9	1.5
1651	-40	0.9	1.5
1715	-30	1.0	1.0
1930	-17	1.6	1.4
2001	-35	1.7	1.4
2114	-19	1.8	1.3
2139	-19	1.6	1.0
0039	-25	1.0	2.7
0133	-50	0.7	2.2
0220	-50	0.4	2.2
0245	-50	1.0	3.5
0321	-50	1.0	5.0
0432	-48	1.0	4.2
0514	-45	0.7	2.2
0542	-48	0.3	2.2
0634	-24	0.3	1.5
0650	-19	0.2	1.7

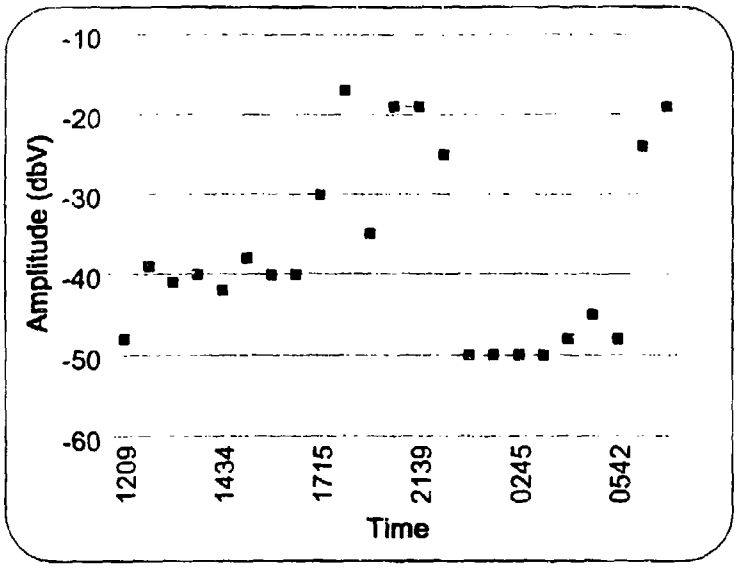

Figure 23. Amplitude vs Time Plot from WWV (9,999 kHz) on 28-29 April 1994.

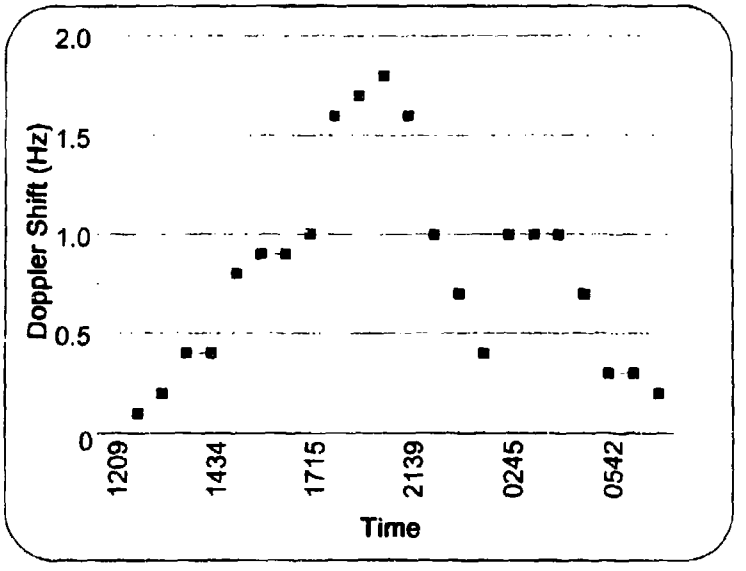

Figure 24. Doppler Shift vs Time Plot from WWV (9,999 kHz) on 28-29 April 1994.

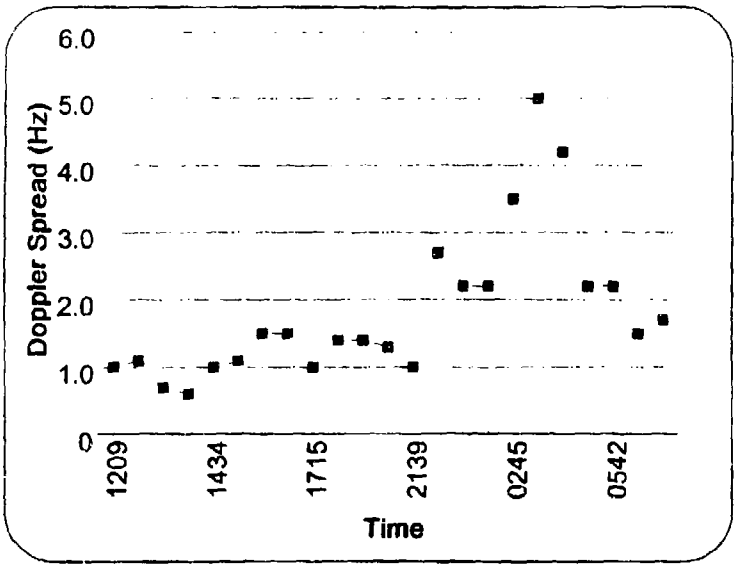

Figure 25. Doppler Spread vs Time Plot from WWV (9,999 kHz) on 28-29 April 1994.

C. 4,999 kHz WWV OBSERVATIONS.

A set of observations of WWV at 4,999 kHz from 1115 to 1543, on 5/4, shown in Figure 26. The signal strength during the day is much weaker than that at 10 and 15 MHz. This is because the lower frequencies are attenuated more in the daytime by the D-layer. The Doppler spread does not change as much or as rapidly for this lower frequency. No significant Doppler shift is observed and the signal amplitude maintains an average value of -60 dBV.

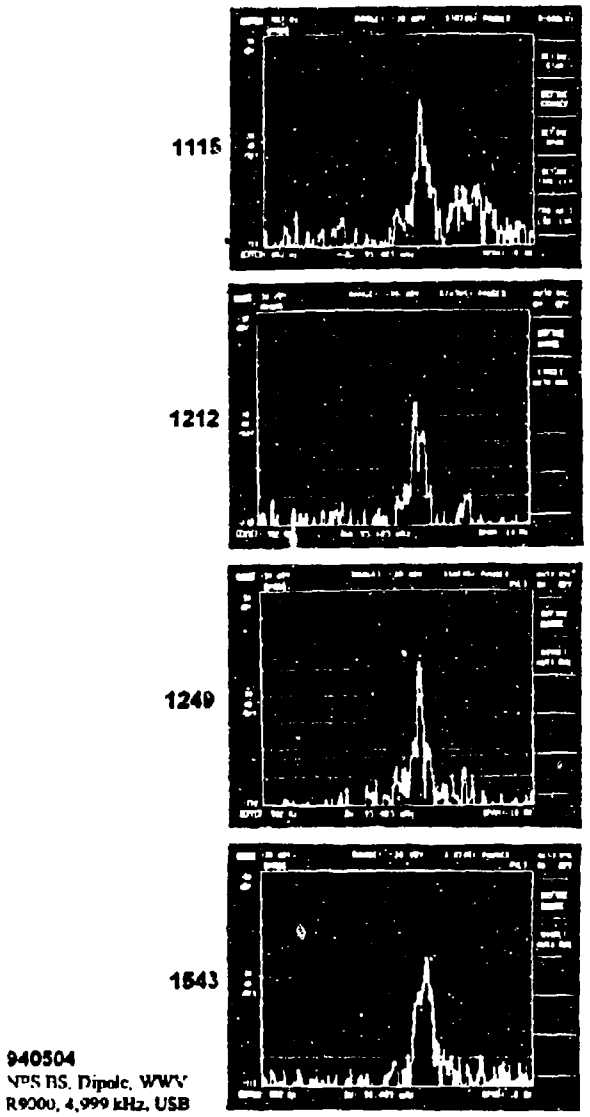

Figure 26. WWV Observations at 4,999 kHz on 4 May 1994.

Figure 27 illustrates the frequency spectra from 1229 to 1946 hours on 4/30. There is a clear increase in the strength and spread of the signal after sunset, as the D-layer

disappears. The amplitude increases about 30 dB, but no significant Doppler shift is observed. The 6 dB spread, starting with a value of 0.2 Hz at 1229 hours, reaches a peak value of 3.5 Hz at 1946.

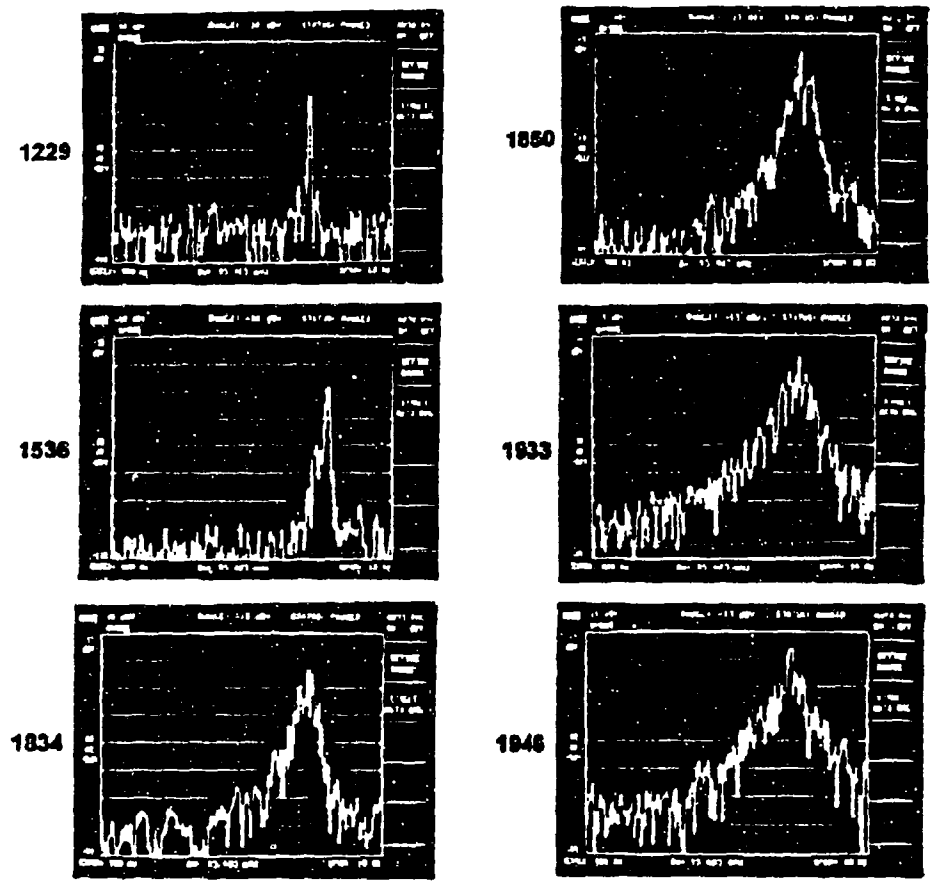

Figure 27. WWV Observations at 4,999 kHz on 30 April 1994.

Between 0608 and 1206 hours on 5/1 (Figure 28), the signal amplitude decreases after sunrise, as the D-layer forms. Throughout the daylight period, the signal drops by 40 dB, with a positive Doppler shift after sunrise.

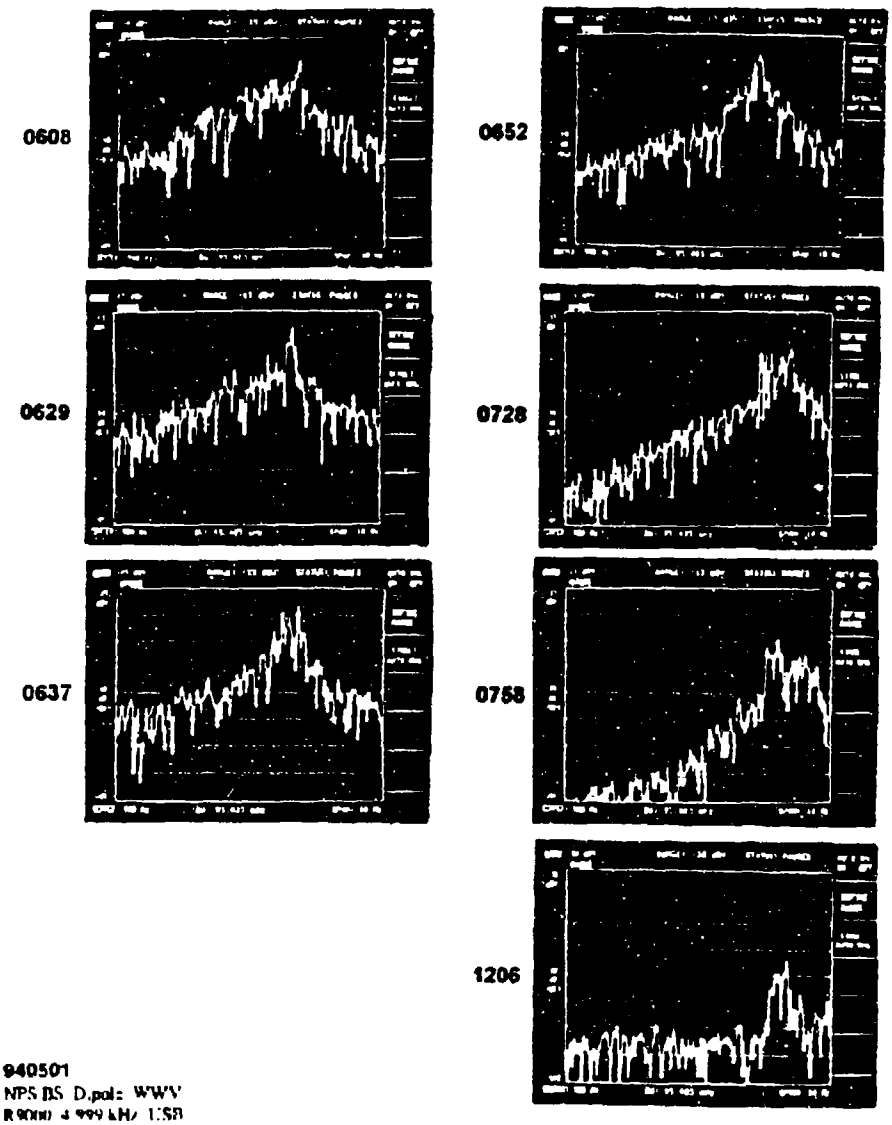

Figure 28. WWV Observations at 4,999 kHz on 1 May 1994.

Tables IV and V summarize the data of 4/30 and 5/1 and plots of amplitude, Doppler shift, and spread variation over the period are in Figures 29-34. Conclusions derived from the above observations are:

- The signal amplitude drops to -40 dBV during the daytime, due to the existence of the D-layer. At night, it increases significantly, peaking at -20 dBV.
- The signal shift is much less at 5 MHz than it is at 10 and 15 MHz. While the signal is stable over most of the period, there is a shift between sunrise and noon of about 1.0 Hz.
- The frequency spectrum spreads around sunset, with 6 dB average values of about 5.0 Hz. After sunrise, the shift is less.

TABLE IV. DATA RECEIVED FROM WWV (4,999 kHz) ON 30 APRIL 1994.

Time	Amplitude (dBV)	Doppler Shift (Hz)	Doppler Spread (Hz) at 6 dB Amplitude
1229	-50	Reference	0.2
1536	-49	0.7	0.9
1834	-27	0.4	2.0
1850	-21	0.2	2.0
1933	-23	0.2	3.3
1946	-22	0.1	3.8

TABLE V. DATA RECEIVED FROM WWV (4,999 kHz) ON 1 MAY 1994.			
Time	Amplitude (dBV)	Doppler Shift (Hz)	Doppler Spread (Hz) at 6 dB Amplitude
0608	-24	Reference	7.0
0629	-21	-0.2	6.5
0637	-23	-0.3	7.0
0652	-24	-0.1	6.2
0728	-30	0.1	5.0
0758	-35	1.0	3.5
1206	-62	1.1	1.7

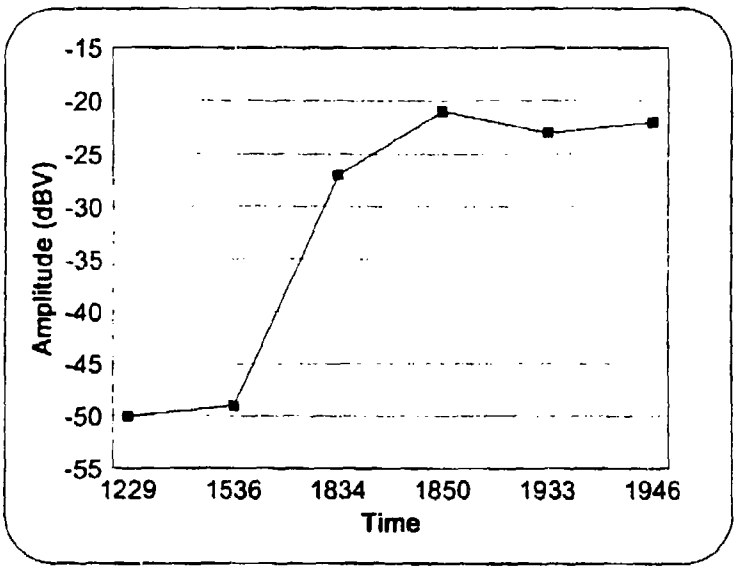

Figure 29. Amplitude vs Time Plot from WWV (4,999 kHz) on 30 April 1994.

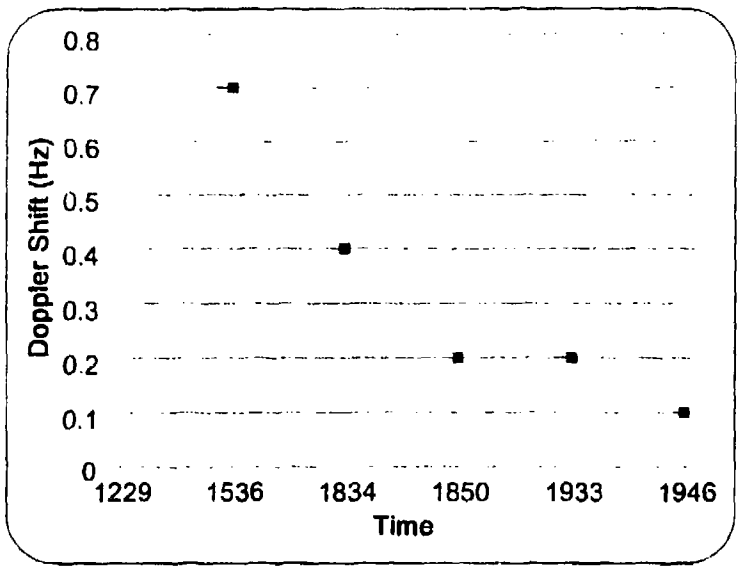

Figure 30. Doppler Shift vs Time Plot from WWV (4,999 kHz) on 30 April 1994.

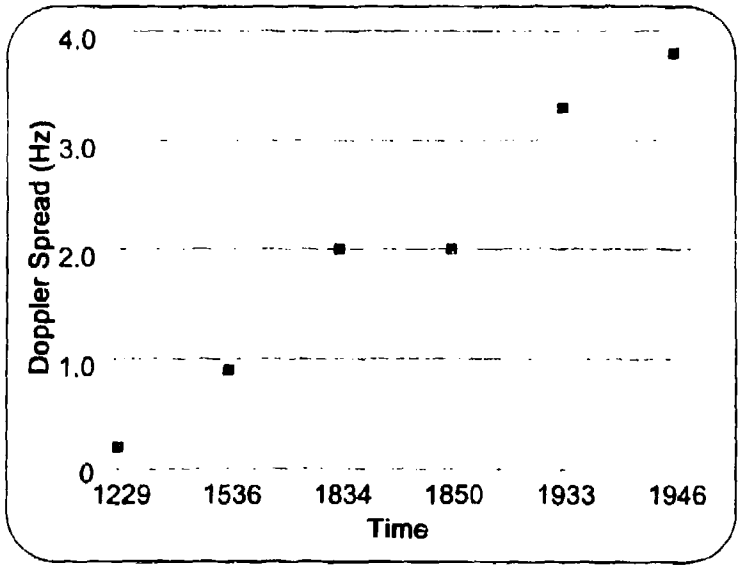

Figure 31. Doppler Spread vs Time Plot from WWV (4,999 kHz) on 30 April 1994.

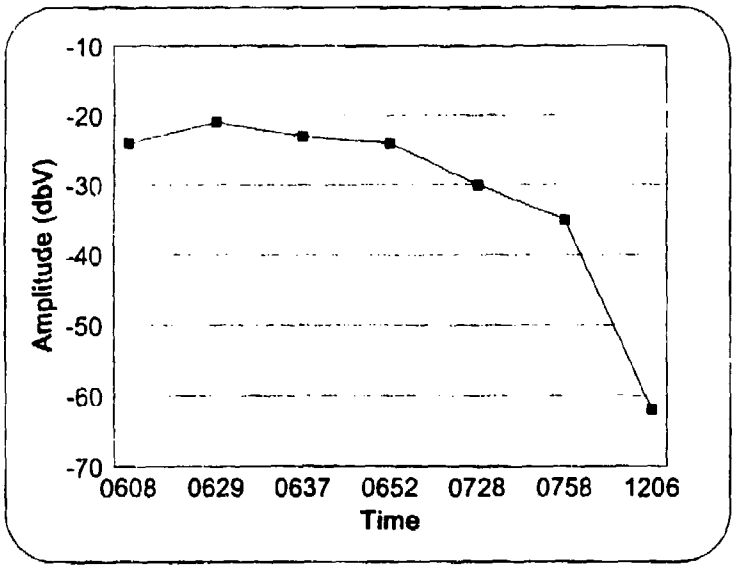

Figure 32. Amplitude vs Time Plot from WWV (4,999 kHz) on 1 May 1994.

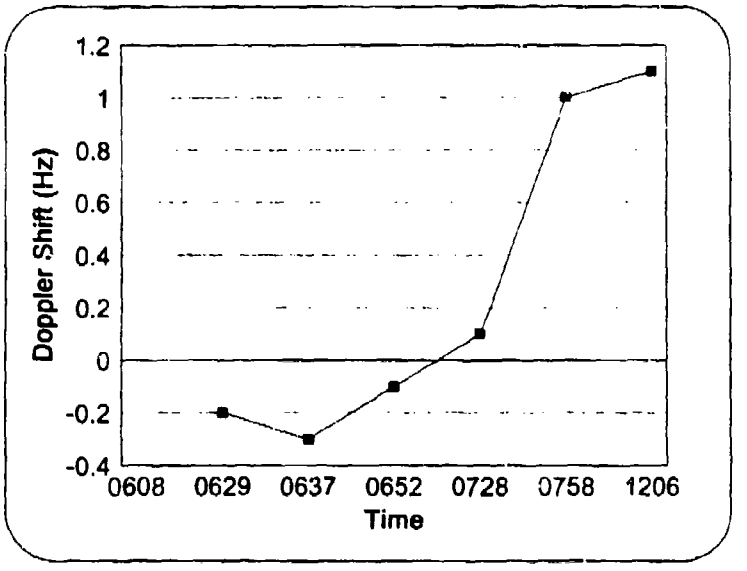

Figure 33. Doppler Shift vs Time Plot from WWV (4,999 kHz) on 1 May 1994.

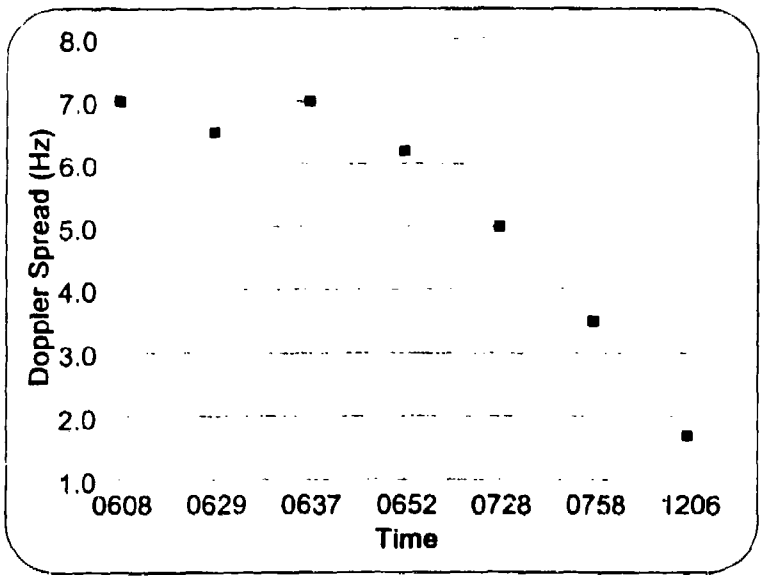

Figure 34. Doppler Spread vs Time Plot from WWV (4,999 kHz) on 1 May 1994.

D. 6,175 kHz BBC RELAY (CANADA) OBSERVATIONS

The next observations cover typical frequency spectra obtained from the BBC Relay Canada broadcasting at a frequency of 6,175 kHz, over a much longer path than for the WWV signals.

The above stations transmit daily from 1600 to 2030 (Pacific Time). Figure 35 covers the time period from 1706 to 2000 on 4/28. At 1706 the signal amplitude is minimum (-65 dBV) and reaches a maximum value of -25 dBV at 1934. At 1934 and 2000 the signal is more spread with a 6 dB value of approximately 6.5 Hz, with some additional spectral components appearing. Doppler shift is negligible throughout the period. Table VI summarizes data from the above observations, while Figures 36 and 37 illustrate variations in amplitude and spread.

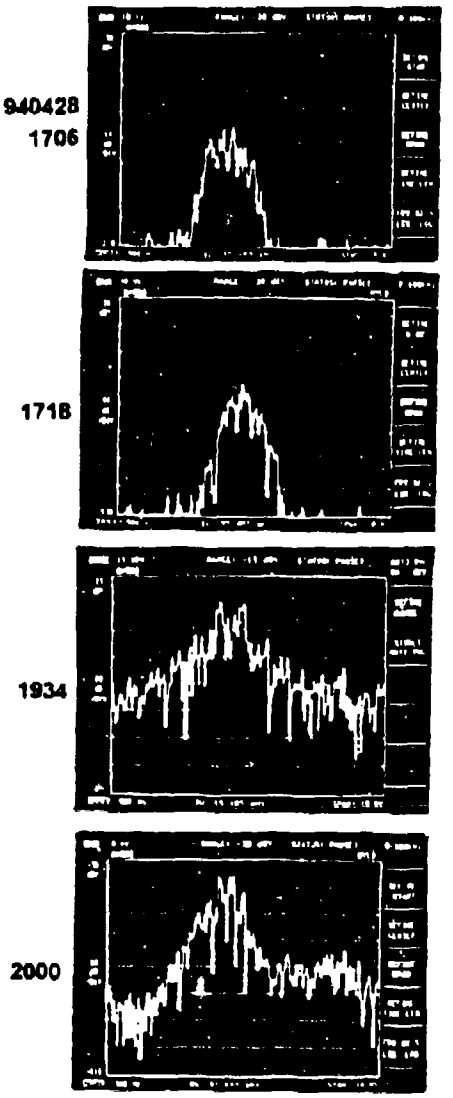

Figure 35. BBC Relay Observations at 6,175 kHz on 28 April 1994.

TABLE VI. DATA RECEIVED FROM BBC RELAY (6,175 kHz) ON 28 APRIL 1994.		
Time	Amplitude (dBV)	Doppler Spread (Hz) at 6 dB Amplitude
1706	-66	2.0
1718	-62	2.1
1934	-25	6.0
2000	-40	6.8

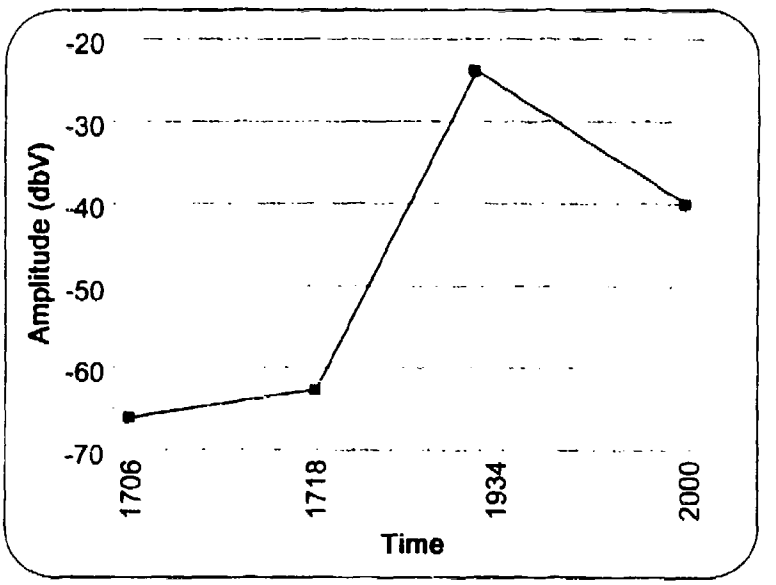

Figure 36. Amplitude vs Time Plot from BBC Relay (6,175 kHz) on 28-29 April 1994.

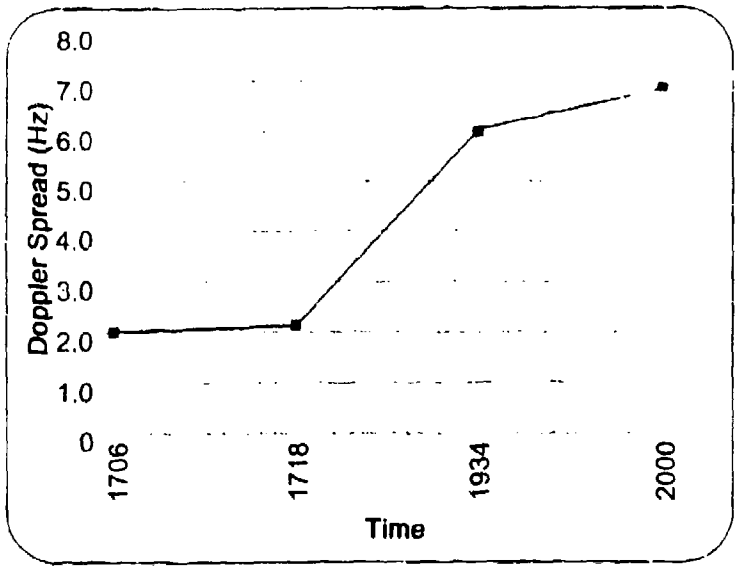

Figure 37. Doppler Spread vs Time Plot from BBC Relay (6,175 kHz) on 28-29 April 1994.

E. 15,260 kHz BBC RELAY (ASCENSION ISLAND) OBSERVATIONS

A signal from the BBC Relay, Ascension Island was monitored from 1319 to 1929 on 4/22. This relay transmits from noon until evening, but not at night. As observed in the Figure 38, the signal experiences a total shift of about 0.8 Hz. The amplitude increases to -38 dBV at 1856 hours when the maximum 6 dB spread of 4.0 Hz occurs.

Table VII contains data for the above observations. Signal amplitude, shift, and spread variations are illustrated in Figures 39, 40, and 41, and are summarized as:

- The total variation in signal amplitude is approximately 30 dB.
- The spectrum spreads most in the afternoon, with an average 6 dB value of 3.5 Hz.
- A total frequency shift of about +0.8 Hz is present.

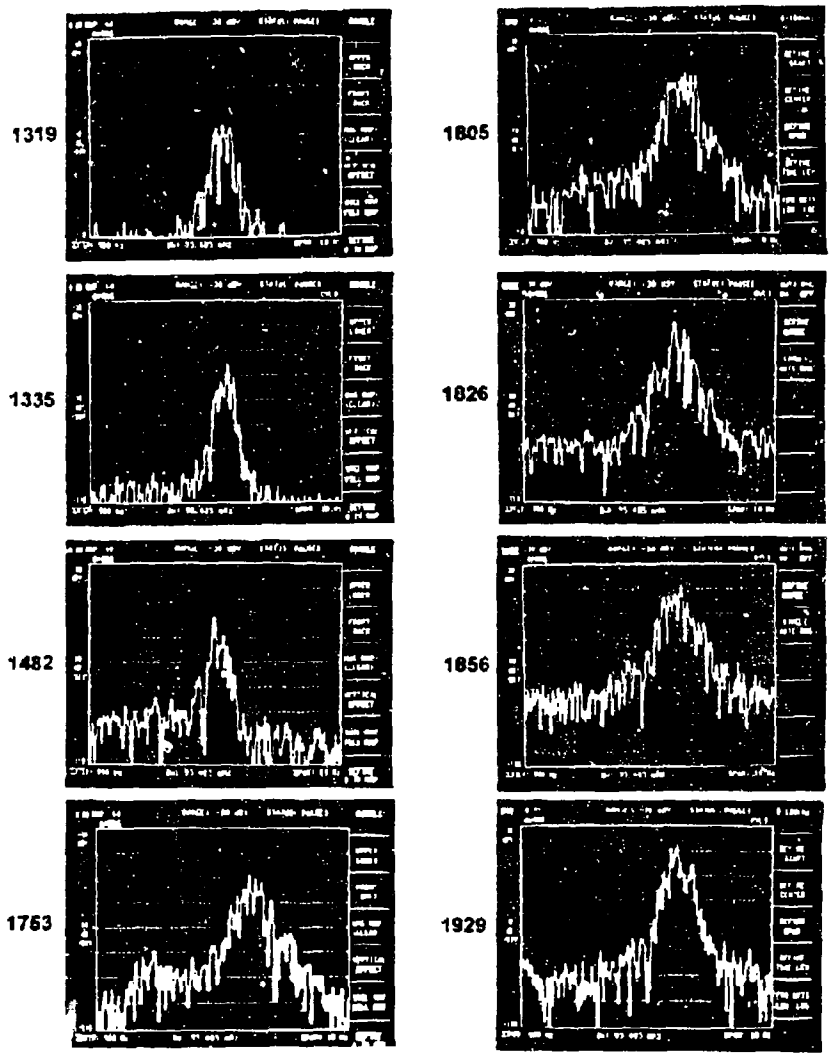

Figure 38. BBC Relay Observations at (15,260 kHz) on 22 April 1994.

TABLE VII. DATA RECEIVED FROM BBC RELAY (15,260 kHz) ON 22 APRIL 1994.			
Time	Amplitude (dBV)	Doppler Shift (Hz)	Doppler Spread (Hz) at 6 dB Amplitude
1319	-66	0	1.2
1335	-55	0	1.1
1482	-50	-0.5	1 6
1753	-49	0.5	3.0
1805	-48	0.4	3.1
1826	-39	0.5	2.6
1856	-39	0.6	3.0
1929	-39	0.5	2.0

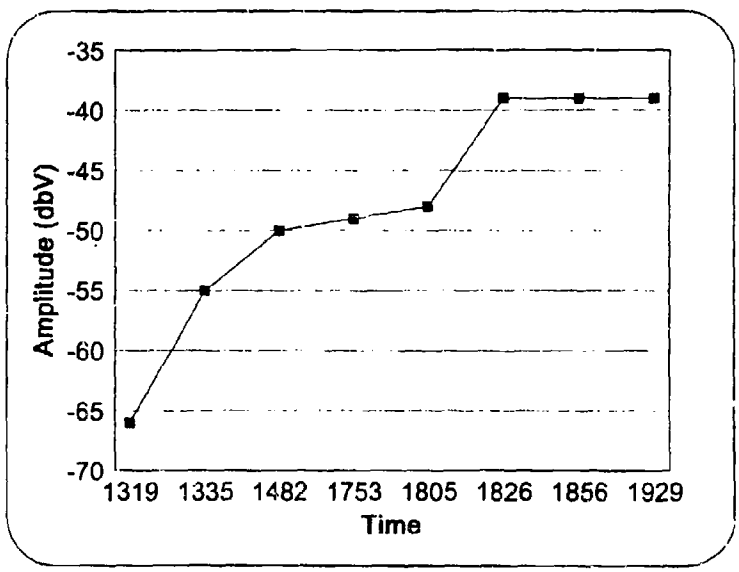

Figure 39. Amplitude vs Time Plot from BBC Relay (15,260 kHz) on 22 April 1994.

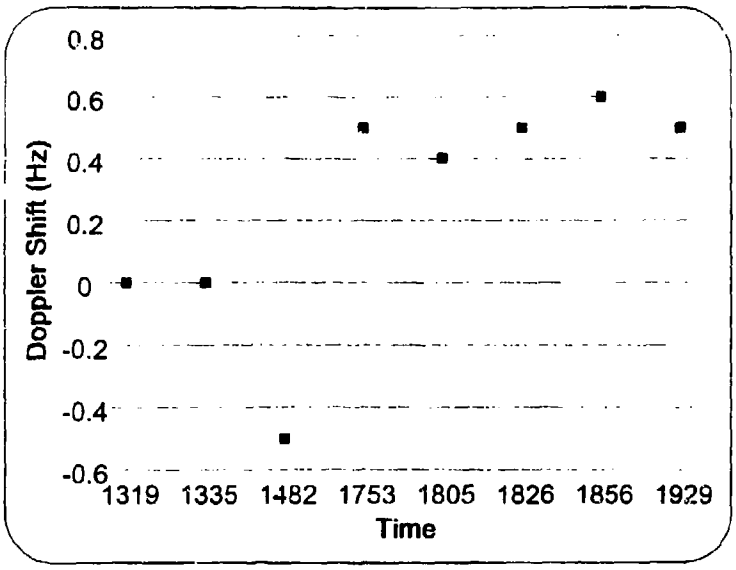

Figure 40. Doppler Shift vs Time Plot from BBC Relay (15,260 kHz) on 22 April 1994.

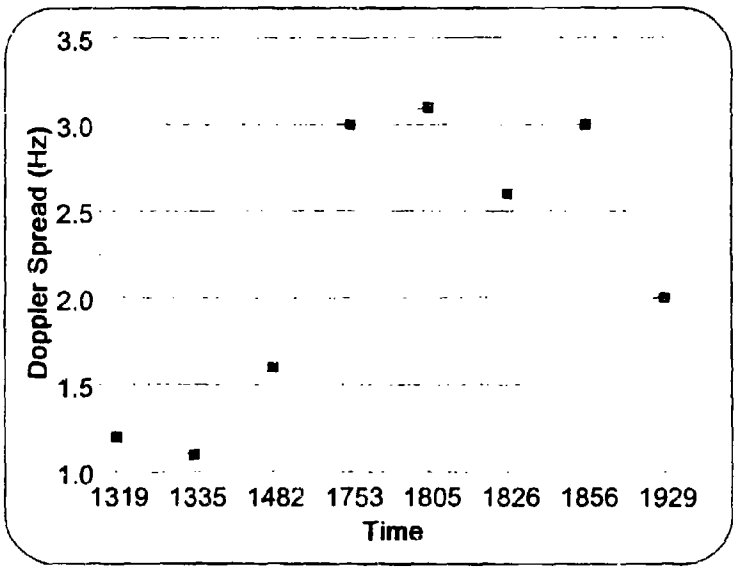

Figure 41. Doppler Spread vs Time Plot from BBC Relay (15,260 kHz) on 22 April 1994.

F. 16,804 kHz CAPE WALES, AK (NAF) OBSERVATIONS

Figure 42 illustrates a typical example of Doppler spread on a signal transmitted from the Cape Wales, AK Naval Station. The signal was received at Fairbanks, AK on 4/28 and recorded with a precision digital recorder. The digitally recorded data was replayed into the HP 3561A spectrum analyzer and examined in a manner similar to all other data.

While the signal amplitude did not vary significantly from view to view, the Doppler spread changed significantly over very brief intervals of only a few seconds or less. The 6 dB Doppler spread values were as high as 40 Hz. This is because the signal propagation path passed through the disturbed ionosphere associated with the auroral oval, as shown in Figure 43 of the Appendix.

DOPPLER SPREAD — CAPE WALES TO FAIRBANKS

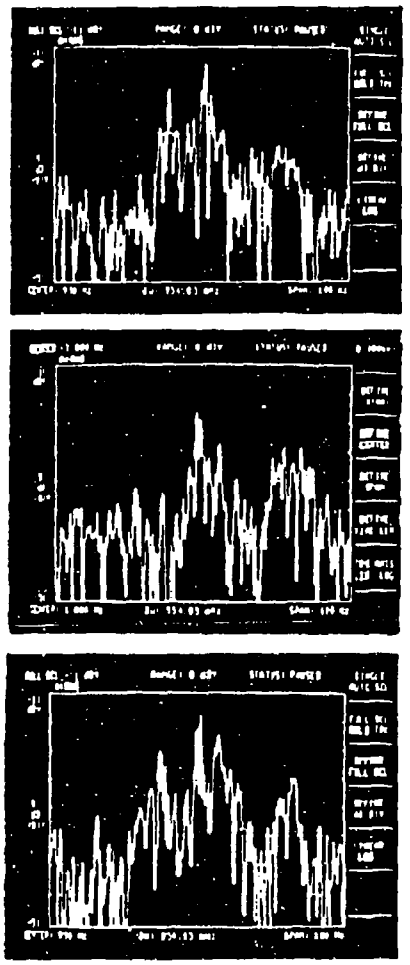

Figure 42. Cape Wales Observations (16,804 kHz) on 8 April 1994.

V. CONCLUSIONS AND RECOMMENDATIONS

A. CONCLUSIONS

In this study the amplitude, frequency shift, and spread variation for the signals of WWV CO (at 5, 10, and 15 MHz), BBC Relay Canada, BBC Relay Ascension Island (at 15,260 kHz), and Cape Wales, AK (at 16,804 kHz) have been examined. The signals were observed at the Naval Postgraduate School and in Fairbanks, AK from 4/5 to 5/10. Figures 44 and 45 show the location of the auroral oval when the data was obtained.

1. Signal Amplitude

During the daytime, the lower-frequency signals experience a significant amplitude attenuation compared to those at higher frequencies. The daytime D-layer absorption is the cause. During the night, lower frequency signals increasing amplitude due to the disappearance of the D-layer, while the amplitude of higher frequency signals decreases due to the decreased (nighttime) density of the F-layer. For instance, a typical amplitude value for a WWV signal transmitted at a frequency of 14,999 kHz is around -30 dBV at around noon, while a 4,999 kHz frequency signal has an amplitude of about -55 dBV at the same time. (The effective radiated power for WWV at the three frequencies is the same). A typical amplitude value observed at around 0600 hours (before sunrise) is -25 dBV for a signal transmitted at 4,999 kHz, and -75 dBV for a signal transmitted at 14,999 kHz.

2. Frequency Shift

Higher frequency signals from WWV experience a more significant Doppler shift than the lower frequency ones. This is because, as equation (14) states, the amount of Doppler shift is proportional to the transmitting signal frequency.

The shift observed from BBC relay signals was less than that of WWV. The reasons are:

- Signals traveling through mid-latitude propagation paths are reflected from relatively stable ionosphere layers and do not usually experience significant frequency shift; and
- Multiple reflections may reduce the total amount of frequency shift, because individual layers may move with different velocity and direction.

3. Frequency Spread

The Cape Wales to Fairbanks, AK signal shows the most spread, because the propagation path passed through the auroral oval as shown in Figure 43 (Appendix). This signal was affected by ionospheric polar region anomalies. The signals coming from WWV did not experience any significant spread during the daytime. The reasons are:

- The ionosphere is more stable during the daytime than at night;
- On the particular dates of observation the ionosphere was quiet;
- The path distance between Monterey, CA and Boulder, CO is only a one hop path;
- Because this path experiences no mid-point ground reflection and only a single reflection from the ionosphere, little spreading occurs; and,

- During the nighttime the signals from WWV were more spread because the ionosphere is usually more unstable at night.

Signals from BBC Relays appear to be more spread than those of WWV. The reasons are:

- Due to the longer distances traveled, the wave experiences more than one ionospheric reflection, producing more disturbances in the signal.
- Field-aligned ionization, as found in the polar regions, can support non-great-circle propagation on paths such as the Sackville to Monterey path. The field-aligned ionization is significant during ionospheric storms, but it still exists to some extent during quiet times. Field-aligned ionization changes rapidly with time and causes severe Doppler effects during ionospheric storms and mild Doppler effects during quiet times.

B. RECOMMENDATIONS

Recommendations for further research are:

- Repeat the experiments over a longer period of time, so that seasonal variations in the signals' frequency spectra can be observed; and
- Repeat the experiments during disturbed ionospheric conditions so that the received data can be compared to those obtained in this thesis, when the ionosphere was relatively quiet (maximum value of K_p was 4).

APPENDIX: AURORAL OVAL POSITION PLOTS

This Appendix contains Figure 43, 44, and 45, showing the auroral oval position on 4/8 at 1000 (UT) hours, 4/29 at 1100 (UT) hours, and 4/29 at 0300 (UT) hours. Plots were obtained using ADVANCED PROPHET program, version 4.3.

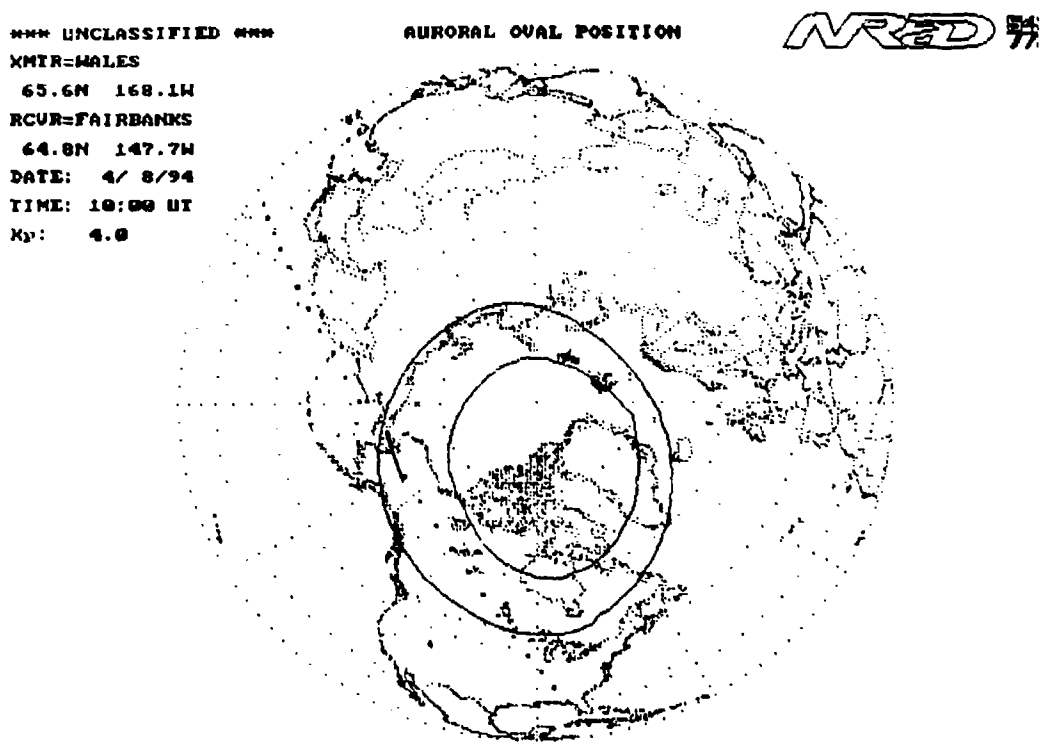

Figure 43. Map Showing the Auroral Oval Position on 4/8 1000 (UT) and the Propagation Path from Cape Wales, AK to Fairbanks, AK.

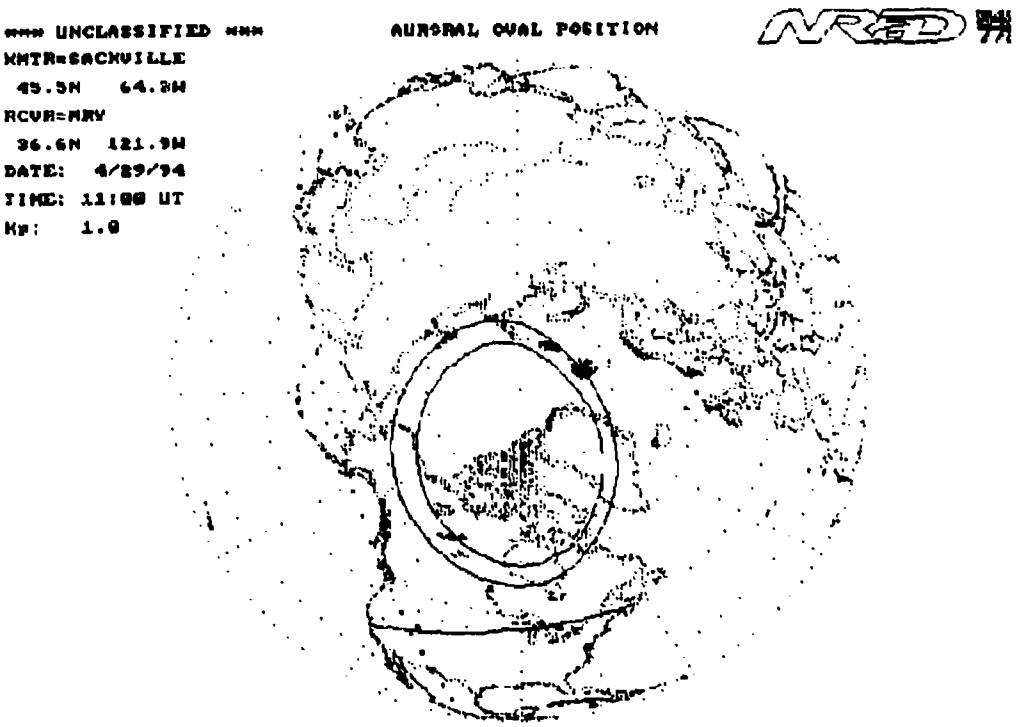

Figure 44. Map Showing the Auroral Oval Position on 4/29 1100 (UT) and Propagation Path from Monterey, CA to Sackville, Canada.

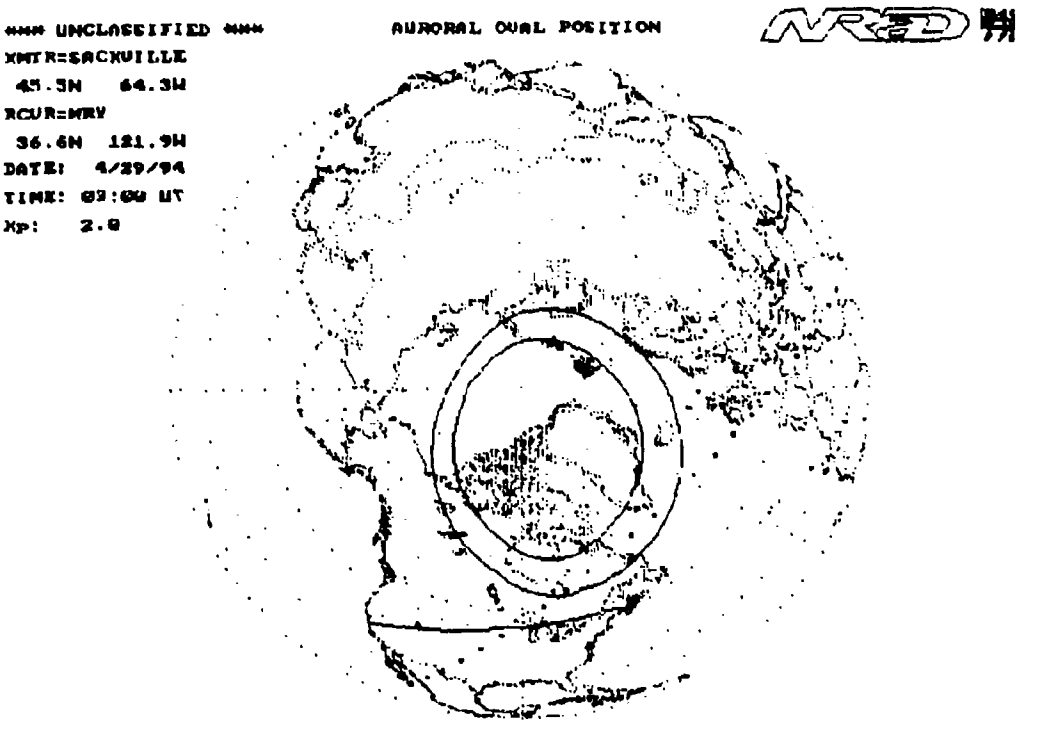

Figure 45. Map Showing the Auroral Oval Position on 4/29 0300 (UT) and Propagation Path from Monterey, CA to Sackville, Canada.

LIST OF REFERENCES

1. John M. Goodman, *HF Communications Science and Technology*, Van Nostrand Reinhold, New York, 1992.

2. Rasler W. Smith, *Ionospheric Effects on Precision Frequency Measurements*, Master's Thesis, Naval Postgraduate School, Monterey, CA, 1990.

3. Bullington, Kenneth, "Radio Propagation Fundamentals," Figure 17, p. 620, *The Bell System Technical Journal*, May 1957.

4. Shen, Frances F., *Introduction to Plasma Physics and Control Fusion, Vol. I: Plasma Physics*, Plenum Press, 1983.

5. Maslin, Nickolas, *HF Communications, a System Approach*, Plenum Press, New York, 1987.

6. McNamara, Leo and Roger Harrison, "Radio Communicators Guide to the Ionosphere," *Australian Electronics Monthly*, pp. 73-80, June 1986.

7. Budden, K.G., *The Propagation of Radio Waves*, Cambridge University Press, Cambridge, 1985.

8. Picketing, Leslie W., "The Calculation of Ionospheric Doppler Spread on HF Communication Channels," *IEEE Trans. on Communications*, Vol Com-23, No. 5, May, 1975.

9. Rose, R.B., *Ionospheric Experimentation-Quarterly Report Number 2*, NOSC Project SY49, NOSC, San Diego, 1989.

10. World Radio TV Handbook, BPI Communications, 1515 Broadway, New York, NY 10036.

11. Myers, Glen A., "Doppler Shift Viewed as a Result of Variable Delay," *The Physics Teacher*, pp. 284-285 May, 1988.

12. McNamara, Leo and Roger Harrison, "Radio Communicators Guide to the Ionosphere," *Australian Electronics Monthly*, pp. 99-106, October, 1985.

13. Reference Data For Engineers: Radio, Electronics, Computer, and Communications, Edward C. Jordan, ed., Howard W. Sams and Co., A Division of Macmillan, Inc., 4300 West 62nd Street, Indianapolis, IN 46268.

INITIAL DISTRIBUTION LIST

1. Defense Technical Information Center — 2
   Cameron Station
   Alexandria, VA 22304-6145

2. Library, Code 52 — 2
   Naval Postgraduate School
   Monterey, CA 93943-5101

3. Chairman, Code EC — 1
   Department of Electrical and Computer Engineering
   Naval Postgraduate School
   Monterey, California 93943-5121

4. Professor Richard W. Adler, Code EC/Ab — 5
   Department of Electrical and Computer Engineering
   Naval Postgraduate School
   Monterey, California 93943-5121

5. Professor Wilbur R. Vincent, Code EC/Ab — 3
   Department of Electrical and Computer Engineering
   Naval Postgraduate School
   Monterey, California 93943-5121

6. Chris Adams — 1
   ManTech
   6593 Commerce Ct.
   Gainsville, VA 22065

7. Roy Bergeron — 1
   ERA
   1595 Spring Hill Rd.
   Vienna, VA 22180

8. Anne M.G. Bilgihan — 1
   USA INSCOM MSA-V EAQ
   Bldg 160 MS Vint Hill Farms
   Warrenton, VA 22186-5160

9. George Hagn 1
SRI International
1611 N. Kent St.
Arlington, VA 22209

10. CDR Gus Lott 1
Naval Security Group Command, Code GX
3801 Nebraska Ave. NW
Washington, DC 20393-5210

11. George F. Munch 1
160-CR-375
San Antonio, TX 78253

12. Jane Perry 1
1921 Hopefield Rd.
Silver Spring, MD 20904

13. Dr. James K. Breakall 1
Penn State University
306 EE East
University Park, PA 16802

14. Dr. Robert Hunsucker 1
R P Consultants
1618 Scenic Loop
Fairbanks, AK 99709

15. George Lane 1
Voice of America/ESBA
300 Independence Ave. SW
Washington, DC 20547

16. Robert Riegel 1
SR 177B
Ridge, MD 20680

17. Dennis Sheppard 1
Naval Security Group Command/Code GX
3801 Nebraska Ave. NW
Washington, DC 20393-5220

18. Dr. A.J. Ferraro
Penn State University
Ionosphere Res. Lab
University Park, PA 16802 — 1

19. Dr. John K. Hargreaves
University of Lancaster/E.S. Dept.
Bailrigg, Lancaster, UK LA2 8LL — 1

20. William Hickey
156 Barcelona Dr.
Boulder, CO 80303 — 1

21. Wayne Bratt
NOSC, Code 772
271 Catalina Blvd
San Diego, CA 92152-5000 — 1

22. Peter Bradley
Rutherford Appleton Lab
Chilton, Didcot, Oxon
UK, OX11 OQW — 1